中国激光

光学显微成像助力肿瘤精准医疗

杨彬，岳蜀华，王璞*

北京航空航天大学生物与医学工程学院，北京市生物医学工程高精尖创新中心，北京 100083

摘要 精准医疗是当下肿瘤诊疗的核心问题，即针对不同的病人定制治疗方案，以获得更好的治疗效果和预后。因肿瘤生物机制及诊疗方案的复杂性，现行基于基因测序和传统表型功能检测的肿瘤精准医疗临床实践，难以有效制定可覆盖大部分病患和药物选择的治疗方案。光学显微成像技术能够对肿瘤组织和细胞中的基因组、蛋白组和代谢组信息进行定量分析和空间定位，识别特定病患肿瘤分子特征和生化反应异常，从而建立起肿瘤基因组和表型组的认知桥梁。本文介绍了不同光学显微成像技术在肿瘤精准医疗领域的相关研究和应用，包括多重免疫荧光（mIF）、荧光原位杂交（FISH）和相干拉曼散射（CRS）等光学显微成像技术。这些技术可以从肿瘤微环境、分子特征和代谢组学等角度进行深入洞察，在肿瘤精准医疗领域发挥着重要作用。

关键词 肿瘤精准医疗；二代测序；表型功能检测；光学显微成像；相干拉曼散射；中红外光热成像

中图分类号 O437.3 **文献标志码** A **DOI**：10.3788/CJL240447

1 引 言

过去几十年中，研究者在肿瘤研究领域[1-2]付出了巨大努力，在肿瘤的诊断[3-4]和治疗[5-12]方面均取得了实质性进展，但肿瘤目前仍是世界范围内最主要的健康问题。针对特定病人制定精准有效的诊疗方案，即肿瘤精准医疗的更深入实践，是当务之急。肿瘤精准医疗，即通过分析个体肿瘤患者的基因型和分子图谱等信息，将最合适的治疗方案与个体最大疗效相匹配，未对其实现路径作任何限制。但是，随着研究者对肿瘤遗传学的不断探索，尤其是二代测序（NGS）在靶向药物伴随诊断中的应用，目前呈现出了一种将肿瘤精准医疗与基于测序的诊断等同起来的趋势。

当前，大多数为患者匹配治疗方案的努力都依赖于测序技术。二代测序技术的显著进步使肿瘤生物学家能够识别肿瘤的数万种突变，其中部分突变的促癌功能已被阐明，这些突变可被当作肿瘤相关生物标志物来辅助治疗。然而，在临床场景下的肿瘤病例中，能够引起肿瘤的基因比已经阐明机理的致癌基因要多得多，同时，从基因突变到肿瘤表型的传导网络异常复杂，众多致癌突变导致肿瘤发生的生物机制还远未阐明。虽然靶向用药的临床试验研究是肿瘤精准医疗的代表性创新方法，但基于测序结果进行伴随诊断的患者队列只有11%～23%获得了预期的治疗反应[13-15]。面对动态且呈网络状交织的突变的影响，仅依据静态的测序结果难以对肿瘤临床诊疗进行有效的精准指导。鉴于肿瘤成因和亚型的复杂性，如何将不断涌现的靶向、免疫以及联合用药方案切实有效地应用于临床实践，已成为临床医生面临的重大挑战。

大多数患者需要新的且与基因测序具有互补性的策略来匹配合适的治疗方案。在当前的肿瘤临床用药筛选实践中，最具吸引力的方案是表型功能检测，即通过识别类器官等病源肿瘤模型的细胞活性和增殖状态来评估特定患者对相应治疗干预的适用性和脆弱性。尤其是基于多种光学显微成像技术的肿瘤生物分子分析等方法，突破了老一代表型功能检测往往仅对细胞活性和增殖状态进行检测的局限。利用光学显微成像技术，研究者不但可以对肿瘤组织微环境和糖脂代谢等细胞生理特点进行观测，还可以对特定蛋白进行空间定位并实现对相关酶活性的定量分析，从而识别肿瘤分子特征和生化反应异常，为肿瘤精准医疗提供除基因型外更多维度的单细胞和分子生物学信息。因而该技术有望成为理解肿瘤基因型和表型的桥梁。

2 现行肿瘤精准医疗应用的局限

2.1 基于基因组学的肿瘤精准医疗

首个人类基因组序列[16]发表（2004年）后，2005年第一个大规模并行DNA测序平台出现，开创了下一代测序（NGS）[17-18]的新时代，并使得在相对较大的临床队列中对全基因组进行测序以识别罕见突变成为可能。研究者借助高通量全基因组测序可以发现肿瘤基因组中的诸多致癌变异，从而可以进行个体致癌突变检测以及基于此的个性化肿瘤诊疗[26-27]，该范式已在不同临床场景中成功应用[28-30]。同时，许多研究报道

收稿日期：2024-01-03；**修回日期**：2024-03-06；**录用日期**：2024-03-19；**网络首发日期**：2024-03-29

通信作者：*10318@buaa.edu.cn

显示，可通过外显子组测序来识别多种遗传性疾病[31-32]和肿瘤[33-42]的致病突变，其中的特定序列区域将被测序数百甚至数千次，以实现高灵敏度[43-44]。

转录组测序技术（RNA-Seq）可以提供细胞和组织在不同生理状态下的基因表达和调控模式快照。虽然转录组只代表人类基因组的一小部分（<5%）[45]，但来自选择性剪接[46]、基因融合[47]、反义转录[48]和RNA编辑[49]的转录本在很大程度上增加了转录组的多样性。RNA-Seq可以检测等位基因特异性表达、融合转录本和非编码RNA可能会导致肿瘤的基因表达异常，因此被越来越多地应用于肿瘤研究，极大地促进了列腺癌[50-55]、乳腺癌[56-57]、淋巴瘤[58-59]、肉瘤[60]和黑色素瘤[61]等各类肿瘤中新基因表达突变的发现。

尽管目前为患者匹配治疗方法的大部分努力都依赖于测序技术，而且新一代测序（NGS）技术的显著进步使得肿瘤生物学家能够识别数万个促癌突变[62-63]，但人们也正在接近致癌突变的“长尾”，即大多数易被解释的肿瘤驱动突变已经被发现；同时，到目前为止，基于测序指导的临床治疗效果并未普遍重现伊马替尼在慢性髓系白血病（CML）患者中实现>90%应答率的优异表现[64-65]，更多的情况是只有一小部分（<10%）肿瘤患者能够受益于基因突变靶点相对应的治疗[66]。显然，仅通过基因测序难以全面指导肿瘤的精准诊疗。

2.2 基于表型功能检测的肿瘤精准医疗

基因变异传导到肿瘤表型的机制异常复杂且充满了随机性[67]，除了已批准的靶向治疗临床适应证，目前无法有效靶向大多数潜在的肿瘤驱动基因，同时，化疗药物的基因组生物标志尚不明确。因果机制复杂和动静态系统不匹配等缺陷，使得单纯依赖基因组学实现肿瘤精准医疗困难重重。针对该问题，研究者构建了可对肿瘤表型进行检测的患者源异种移植（PDX）小鼠模型。PDX模型理论上保留了患者肿瘤在组织病理学和遗传学上的特征[68-70]，但高昂的价格和低时效性导致其很难被应用到日常临床实践中，而是主要被应用于学术研究和制药开发中。近年来，诸多新兴肿瘤模型的涌现使得表型功能检测突破了传统PDX模型的局限，逐渐成为一个颇具前景的方案（如图1所示），该方案可在低成本且保留病源肿瘤特征的前提下评估肿瘤对治疗干预的脆弱性[71-72]。

近年来，循环肿瘤细胞（CTC）方法取得了显著进

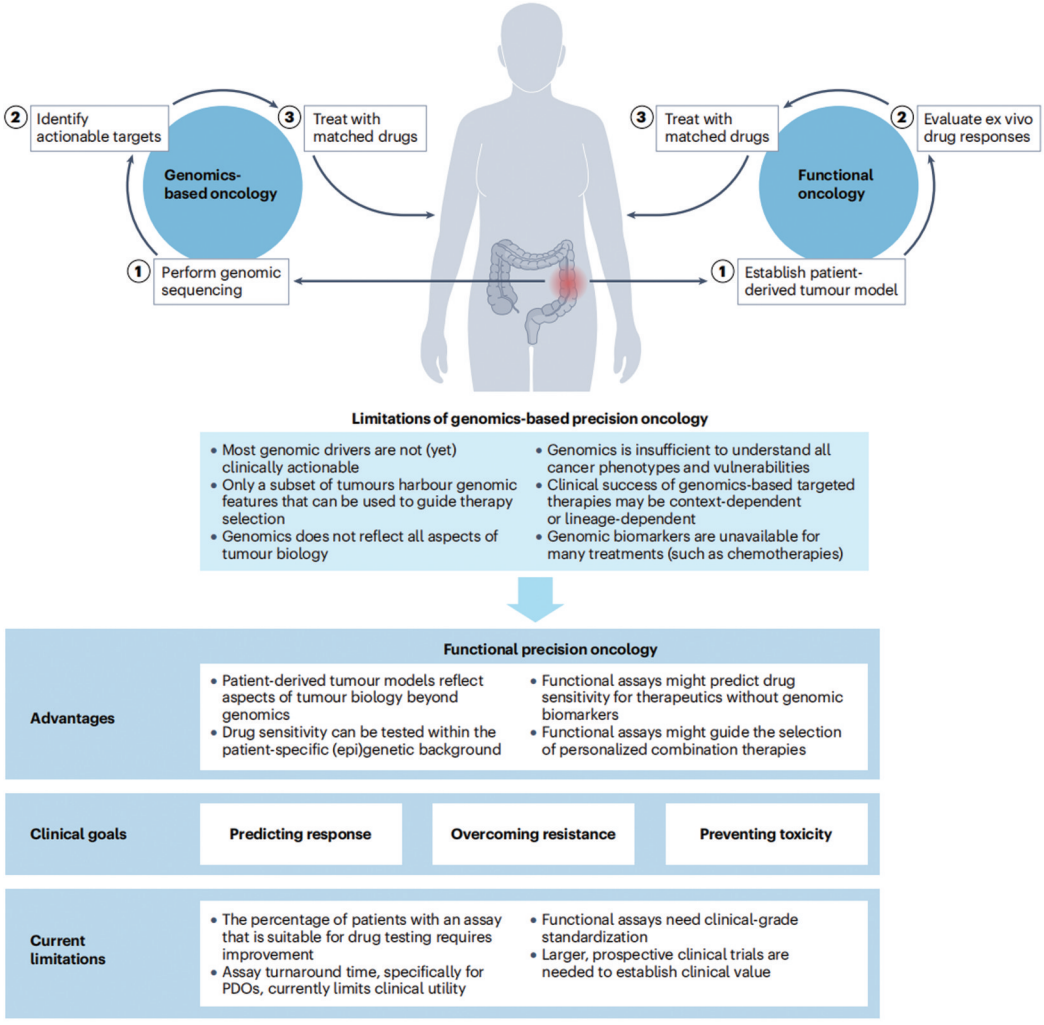

图1 从基因型到表型的肿瘤精准医疗[71]

Fig. 1 Genomics-based precision oncology to functional precision oncology[71]

步。以前需要立即将CTC移植到动物体内进行繁殖，即便如此，成功率也很低。使用改进的CTC微流控芯片从乳腺癌患者肿瘤中分离出CTC，接着通过扩展便可使更广泛和更深层次的功能检测及测序成为可能[73]，但其缺点是缺乏与亲代肿瘤类似的微环境。为提供与真实肿瘤微环境（TME）相似的异质相互作用，研究人员开发出了包含多种细胞类型的人工器官型培养物，这些培养物的基因表达模式与亲代肿瘤更具一致性[74]。这种基于多种细胞系重构的培养模型已被证明可以预测体内结果[75]。将胃癌和结直肠癌肿瘤病源细胞与成纤维细胞及间质细胞联合进行肿瘤细胞簇（PTC）培养，可在2～3周内完成基于细胞活性和增殖表型的药敏检测，并且准确率可以达到90%[76]。类似的研究模型还有肿瘤薄片[77]和肿瘤“微球体”[78]。在这些模型构建过程中，通常把患者来源肿瘤细胞移植到半固体细胞外基质[79]，并进行细胞扩增[80-81]，建立病源肿瘤类器官（PDO）。这类模型可重建肿瘤来源组织的内源性结构，比2D培养更接近体内肿瘤环境。目前，人们已经从胰腺癌[82]、前列腺癌[83]和结肠癌[81]等病源肿瘤中培养出类器官。

上述患者来源肿瘤模型可维持亲代肿瘤中的致癌突变[82]，但都需要数周时间才能产生足够数量的检测样本；同时，其培养成功率较低并且在不同的研究中差异巨大（40%～85%），导致单例检测成本高达数万元，面临巨大的时效性、成本性和准确性挑战（如图2所示）。而且传统的表型功能检测往往局限于对细胞扩增和活性的检测，难以对肿瘤致病机理和分子特征进行深入研究，无法成为理解肿瘤成因的有力工具。

	PDX	CTC	PTC	PDO
Brief	Fresh tumor tissue or tumor cells from patients are orthotopically or subcutaneously transplanted into immunodeficient mice to form tumor models	CTCs refer to tumor cells present in the peripheral blood of cancer patients, which are sorted and cultured for genetic typing and functional characterization	Tumor tissue is dissociated into single cells, and corresponding growth factors are added to form a tumor model that includes both tumor and microenvironment cells through self-assembly	Tumor stem cells and other related cell types are sorted and classified, and induced to form tumor organoid models
Detection Period	2-4 months	1-2 weeks	2-3 weeks	2-4 weeks
Cost	100,000-300,000 RMB	4000-10000 RMB	Not commercialized	50,000-100,000 RMB
Culture Success Rate	20%–80% Significant deviation	50%–90% Significant deviation	85%	40%–80%
DNA Consistency	>80%	Tumor cells>80% No stromal cells	>80%	>80%
RNA Consistency	>80%	Comparable consistency, But upregulation of growth and proliferation signals	Upregulation of growth and proliferation signals, and with downregulation of immune/circulatory system	Significant upregulation of growth and proliferation signals, but with a significant downregulation of immune/circulatory system
High Throughput	No	Yes	Yes	some degree
Subclonal Retention	Yes	No	Yes	Yes
TME	Partially retained	None	Partially retained	Partially retained

图2 主要表型功能检测肿瘤模型[68-83]

Fig. 2 Primary tumor models for phenotype function testing[68-83]

3 光学显微成像在肿瘤精准医疗领域的应用

表型功能检测主要用于观测肿瘤模型的增殖状态或活性，能够跨越突变理解局限和肿瘤发生机制复杂等基因测序面临的障碍。但表型检测难以提供针对肿瘤组织微环境、细胞分子特征和代谢组学等的微观见解，使得研究人员无法结合测序结果对特定病例进行深入的致病和耐药机制探索。并且受检测方式限制，表型检测所需样本量较大，往往需要较长时间的模型培养和构建，导致其对亲代肿瘤表征的一致性低，同时检测周期长、成本高。而产生于活检和手术等临床场景下的肿瘤样本量少，基于有限样本对病源肿瘤进行检测是表型功能检测实现肿瘤精准医疗的前提。新涌现的基于光学显微成像技术的肿瘤生物分子定量分析方法可以解决表型功能检测的局限，即能够高通量多维度地基于有限样本进行检测，其中的一些技术甚至可以用于无损无干扰地观测样本的高时空分辨分子信号，对肿瘤微环境、基因组、蛋白组和代谢分子特征进行深度检测和分析。这些新技术预示着一种有前景的肿瘤诊疗策略，即通过表型检测将蛋白组学、代谢组学信息与测序结果相结合，从而将最佳疗法匹配到特定的肿瘤患者，并对深层致病机制进行探讨（如图3所示）。比如，Qi等[84]通过基因组和代谢轮廓分析发现

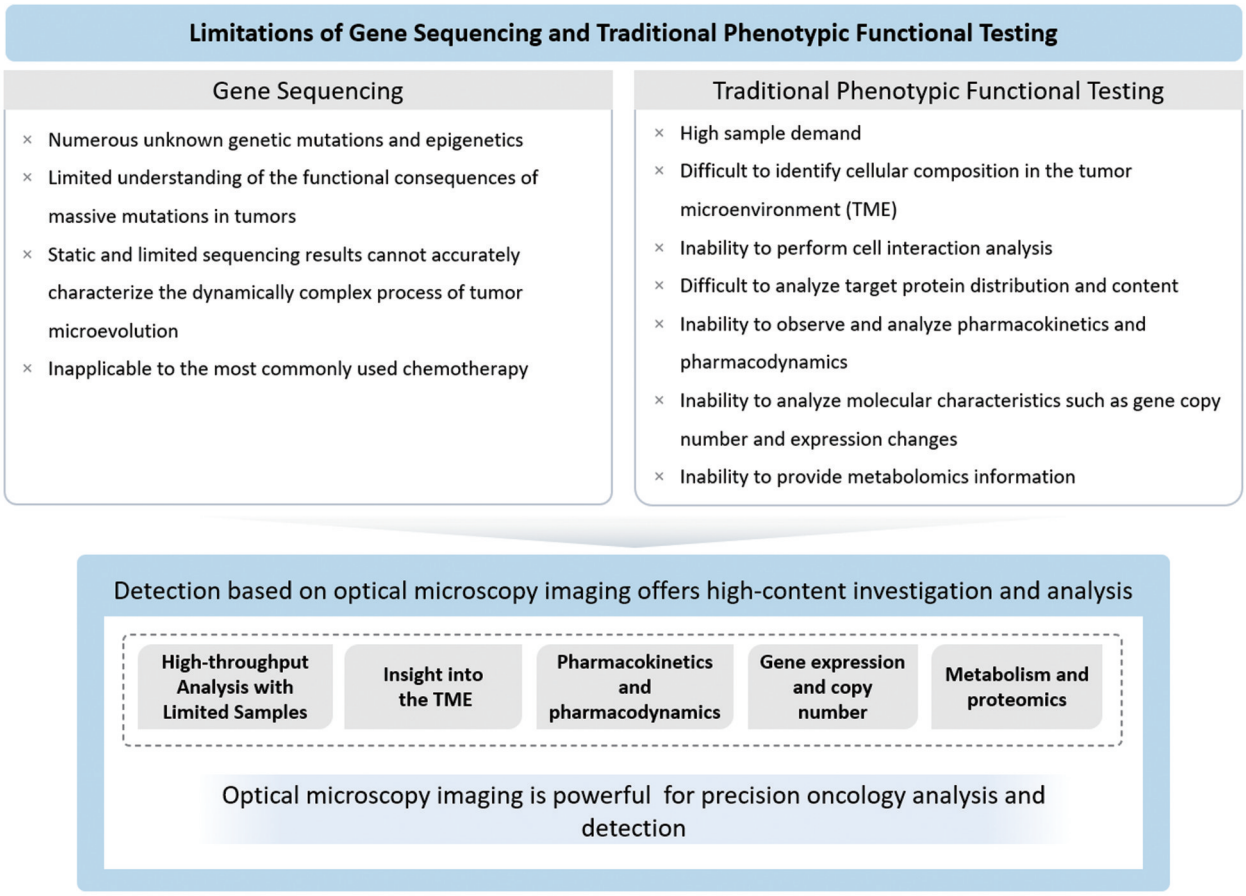

图 3 基于光学显微成像的肿瘤精准医疗优势

Fig. 3 Advantages of tumor precision medicine based on optical microscopy imaging phenotype detection

不同的病患族群在肿瘤代谢和免疫微环境方面存在差异化特征，从而可以根据特定的代谢特征对肝细胞癌患者进行精确有效的治疗。

3.1 多重免疫荧光(mIF)显微成像

免疫荧光成像技术：将不影响蛋白活性的荧光色素标记于抗体或抗原，荧光标记与相应的抗原或抗体结合后，在荧光显微镜下呈现特异性荧光反应，通过荧光色素的发光效应对生物组织和细胞中的特定蛋白进行成像。采用多重荧光探针分别对不同类型细胞的特异生物抗原进行标记，即可区分特定类型的细胞；若采用多重荧光探针对不同类型的目标蛋白分子进行标记，即可对亚细胞目标蛋白的含量和分布进行成像和检测。多重免疫荧光技术和图像数据分析平台的发展，使得人们对肿瘤细胞或组织中不同类型细胞的构成和比例、特定蛋白表达和含量以及空间位置关系等肿瘤微环境信息进行成像和分析成为可能。基于该技术，研究者能够更好地理解肿瘤微环境中的细胞间相互作用，例如对肿瘤免疫治疗有效性起决定性作用的肿瘤浸润淋巴细胞(TIL)。

芬兰赫尔辛基大学的 Launonen 等[85]探讨了 BRCA1/2 突变的高级别浆液性卵巢癌(HGSC)肿瘤微环境(TME)中单细胞免疫表型和空间的相互作用。他们使用多重免疫荧光成像技术，对来自 31 个带有 BRCA1/2 突变和 13 个无同源重组基因改变病历的 112 个肿瘤样本的 124623 个单细胞进行了分析。研究结果揭示了 BRCA1/2 突变肿瘤中免疫监测增强的证据，尤为重要的是该研究展示了增殖性肿瘤细胞亚群的特征及其对预后的影响。在 BRCA1/2 突变肿瘤中，这些亚群的行为与 CD8+、CD4+ T 细胞的空间免疫相互作用关联，通过单细胞空间分析可以证明肿瘤细胞基因型和免疫细胞浸润表型共同影响预后，并为高级别浆液性卵巢癌的免疫治疗策略和患者分层提供新的见解[85]。

基于多重免疫荧光在肿瘤免疫微环境领域的进展，Locke 和 Hoyt[86]将其应用于肿瘤微环境生物标志物的空间相互作用分析，通过数据驱动的方法来深入了解肿瘤与免疫系统的互动。他们提供了一个用于指导空间生物学研究的全面框架(如图 4(a)所示)，该框架通过多重免疫荧光检测到的特征细胞共表达表型来归类患者预后组别，有望提高 PD-1 和其他免疫治疗结果预测的准确性(如图 4(b)所示)。

Taube 等[87]报道了约翰霍普金斯大学、耶鲁大学和安德森癌症中心等 6 家单位进行的基于多重免疫荧光技术指导 PD-1/PD-L1 免疫治疗的跨中心实践，以评估该方法在不同实验室间统计评估的再现性和一致

性。上述研究团队成功地在多个实验室中实现了对PD-1/PD-L1轴的高灵敏和可重复的多重免疫荧光表征，如图4(c)所示。不同的实验室对特定免疫细胞(IC)和肿瘤细胞(TC)的密度、TC上的PD-L1表达百分比(%PD-L1)以及PD-1/PD-L1表达邻近性的检测结果显示出高度一致性，证明了多重免疫荧光技术应用于跨中心临床实践的可行性[87]。

得克萨斯大学安德森癌症中心的Ajani团队研究了YAP1(Yes-Associated Protein 1)在胃腹膜癌(PC)中的作用及其作为治疗靶点的潜力。他们通过双重免疫荧光技术在胃腹膜癌样本中观察到了YAP1和EpCAM的共表达，并发现YAP1高表达的胃腹膜癌细胞具有肿瘤干细胞(CSC)特性，易于在患者源性异种移植(PDX)和类器官(PDO)模型中形成肿瘤。该研究为将YAP1蛋白表达和相关通路上游基因作为胃腹膜癌治疗的新靶点提供了强有力的证据[88]。

南方医科大学的李国新教授团队通过免疫荧光显微成像技术，观察到了MYH9蛋白在胃癌细胞核中的积累，推断MYH9可能参与肿瘤调控基因表达。他们使用免疫荧光共定位技术研究了MYH9与β-连环蛋白在细胞核中的相互作用，明晰了MYH9如何通过与CTNNB1(β-连环蛋白)的相互作用来促进其转录从而影响Wnt/β-连环蛋白信号通路的激活。他们基于免疫荧光显微成像发现MYH9可作为潜在的治疗靶点，特别是在抑制CTNNB1转录和Wnt/β-连环蛋白信号通路激活方面具有重要作用。通过免疫荧光显微成像和染色质免疫沉淀(ChIP)实验，研究者们证实了MYH9可以直接结合到CTNNB1启动子上的特定序列从而促进CTNNB1的转录，发现了MYH9的4个潜在核定位信号(NLSs)，阐述了MYH9促进胃癌细胞无锚生长和转移的机制，这些对于开发抑制胃肿瘤转移的新策略至关重要[89]。

Ijsselsteijn等[90]开发了一种无需酪胺信号放大的免疫荧光方法，该方法通过免疫荧光可同时检测7个关于肿瘤的细胞靶标。2020年，Mori团队[91]描述了其在表征肿瘤免疫微环境方面的工作：他们首先通过标准免疫组织化学和单一复合物IF测试初级抗体，而后开发多重面板，并使用Vectra 3.0多光谱成像系统获得肿瘤组织的免疫微环境图像。2021年，Hoyt[92]采用该方法实现了9重荧光染色的肿瘤组织成像(如图4(d)

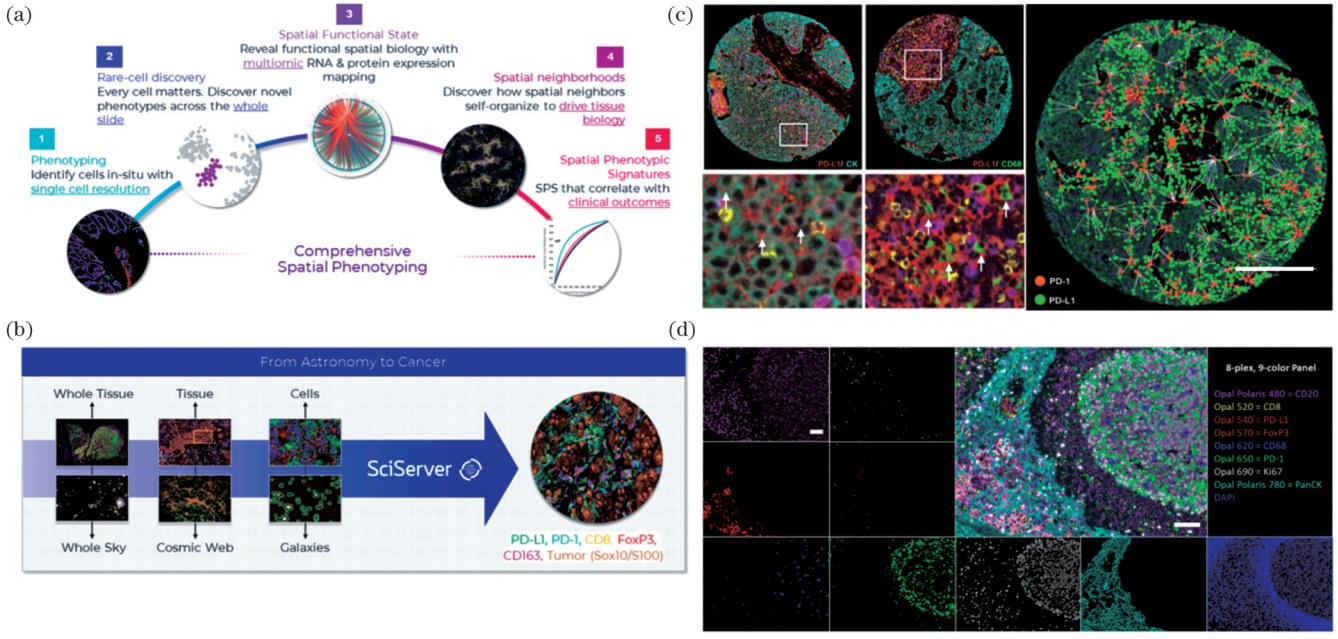

图4 多重免疫荧光成像可深入探查肿瘤微环境和细胞间相互作用。(a)多重免疫荧光满足肿瘤空间生物学研究在不同研究阶段的需求[86]；(b)在肿瘤微环境中通过多重免疫荧光成像识别生物标志物，以预测对免疫治疗的反应[86]；(c)多重免疫荧光对乳腺癌组织微阵列(TMA)中PD-L1共表达的评估对于预测免疫检查点抑制剂治疗的反应具有重要意义[87]，比例尺为200 μm；(d)多重免疫荧光呈现的9色复合图像为研究细胞相互作用及肿瘤微环境提供有力工具[92]，比例尺为100 μm

Fig. 4 Multiplex immunofluorescence (mIF) imaging provides in-depth exploration of the tumor microenvironment and cell-cell interactions. (a) Multiplex immunofluorescence meets the needs of tumor spatial biology research at different research stages[86]; (b) biomarkers can be identified in the tumor microenvironment through multiplex immunofluorescence imaging to predict responses to immunotherapy[86]; (c) assessment of PD-L1 co-expression in breast cancer tissue microarrays (TMA) by multiplex immunofluorescence is significant for predicting responses to immune checkpoint inhibitor therapy[87], with scale bar of 200 μm; (d) 9-color composite images presented by multiplex immunofluorescence provide a powerful tool for studying cell interactions and the tumor microenvironment[92], with scale bar of 100 μm

所示),并讨论了将这种方法转化为临床实践的可能性。值得一提的是,Eminizer等[93]通过对8个黑色素瘤组织样本进行扫描成像,尝试表征和校正三种多光谱显微镜之间光照强度和光谱灵敏度的差异,证明了使用简单的校正模型即可将不同多重免疫荧光显微镜所得的肿瘤组织内细胞共表达谱和空间关系数据进行比较,进一步拓展了多重免疫荧光技术在肿瘤研究领域的应用。

3.2 自发荧光(AF)显微成像

自发荧光成像区别于基于荧光探针的免疫荧光成像,直接对生物体自体和药物来源的自发荧光信号进行成像。自体荧光是细胞结构,如线粒体和溶酶体等,吸收激发光后自然发射的荧光信号。自发荧光成像可以检测生物样本本身或药物来源的具有自发荧光属性的分子的成分、含量和分布,并观测相关生物反应的过程及强度。自发荧光显微成像技术提供了一种直观和非侵入的研究工具,用于评估药物反应和肿瘤异质性,为探察肿瘤样本的多维信息、研究相关药物的药代及药效动力学提供了有力手段。

威斯康星大学麦迪逊分校的Skala等以患者来源的肿瘤类器官(PDOs)作为肿瘤表型检测的研究对象,利用自发荧光显微成像捕捉代谢辅酶NAD(P)H和FAD(黄素腺嘌呤二核苷酸)的自发荧光信号(如图5(a)所示),观察到了PDOs对治疗药物的反应,包括生长抑制和代谢活性的变化,并揭示了PDOs内部的异质性,包括细胞间和类器官间的代谢差异。这种技术能够提供对药物效果的定量评估,有助于识别对特定治疗敏感或耐药的细胞亚群。基于自发荧光成像,医生可以在细胞维度更好地探索和理解不同患者肿瘤的生物学特性,从而为患者选择最合适的治疗方案[94]。

澳门大学Deng教授团队[95]基于自发荧光显微成像技术,通过观察细胞内脂褐素的自发荧光变化来监测药物对肿瘤切片样本的影响,实现了3D肿瘤切片培养(3D-TSCs)中药物诱导的细胞凋亡过程的实时观察。该研究证明了自发荧光显微成像技术可被用于高通量药物筛选,即通过观察药物处理的3D肿瘤切片培养模型中脂褐素自发荧光的变化(如图5(b)所示),可以快速筛选出对肿瘤细胞具有高效杀伤作用的药物,这对于加速药物发现、优化治疗方案以及实现肿瘤治疗的个性化具有重要意义。基于前述研究,Yan等[96]利用自发荧光显微成像技术进一步研究了抗肿瘤药物的临床反应。他们通过观察类脂褐素自发荧光的寿命,验证了通过自发荧光寿命成像(FLIM)可以区分细胞凋亡和坏死(如图5(c)所示)。这对于评估药物的治疗效果和毒性具有重要意义,因为不同类型的细胞死亡会被回溯到不同的通路,预示着不同的治疗反应。

此外还有研究发现,探测细胞自发荧光强度和寿命的双光子显微代谢成像(OMI)是一种用于临床前药物开发的颇具前景的工具。2017年,Cannon等[97]利用OMI量化了同一细胞来源异种移植肿瘤的2D细胞系与3D类器官在药物反应中的细胞动态代谢差异。Heaster等[98]证明了代谢辅酶NAD(P)H和FAD的代谢成像荧光强度和寿命可用于量化肿瘤细胞周期。基于此,2019年,他们又探索了头颈癌细胞群内代谢模式的空间异质性[99]。另外,Lukina等[100]使用双光子显微镜和时间相关单光子计数测量了光学氧化还原比(NAD(P)H荧光强度除以FAD荧光强度)以及NAD(P)H和FAD的荧光寿命参数,并探讨了将自荧光代谢辅酶NAD(P)H和FAD的荧光寿命参数作为评估肿瘤细胞对紫杉醇治疗反应指标的可能性。

3.3 荧光原位杂交(FISH)显微成像

荧光原位杂交(FISH)显微成像是一种分子生物学技术,它利用荧光偶联的DNA片段来标记感兴趣的基因组区域,这些标记的DNA片段会与目标DNA序列互补配对并形成杂交体,通过荧光显微镜可以高分辨观测和分析特定基因的拷贝数和空间位置。荧光原位杂交技术在肿瘤精准治疗中发挥着关键作用,它不仅可以通过成像来识别肿瘤的基因型分子特征,还是连接基因型与肿瘤表型的重要研究工具,并为个体化治疗方案选择提供依据。例如,对人类表皮生长因子受体2(HER2)过量表达的乳腺癌患者,通常使用曲妥珠单抗进行靶向治疗[101],而荧光原位杂交技术是目前临床上检测HER2表达水平的主流方案。

荧光原位杂交显微成像检测到的MET扩增在非小细胞肺癌(NSCLC)、胃癌、结直肠癌等多种类型的肿瘤中均有发现,且明确与肿瘤预后相关。斯隆凯特林癌症研究所的Alexander Drilon教授团队[102]应用荧光原位杂交成像技术对MET基因进行标记,并观测了其拷贝数的变化,同时利用标记染色体7的荧光原位杂交探针(CEP7)计算了MET基因与CEP7的比值(如图6(a)所示)。MET扩增水平与MET靶向治疗的敏感性高度相关,在非小细胞肺癌中高级别的MET扩增一般代表着更好的靶向治疗反应。Chrzanowska等[103]通过荧光原位杂交成像技术检测了MET、ALK和ROS1等相关基因在肿瘤细胞中特定的扩增和重排(如图6(b)所示),这些基因的改变是靶向治疗的关键生物标志物。他们基于荧光原位杂交成像的检测结果预测了肿瘤对特定治疗的反应,如对MET抑制剂和ALK抑制剂等的反应。Pawlyn和Davies[104]讨论了荧光原位杂交成像技术在多发性骨髓瘤(MM)个性化治疗领域的应用,并采用该技术识别了导致骨髓瘤发生和发展的基因重排事件,据此可选择最合适的治疗方案。

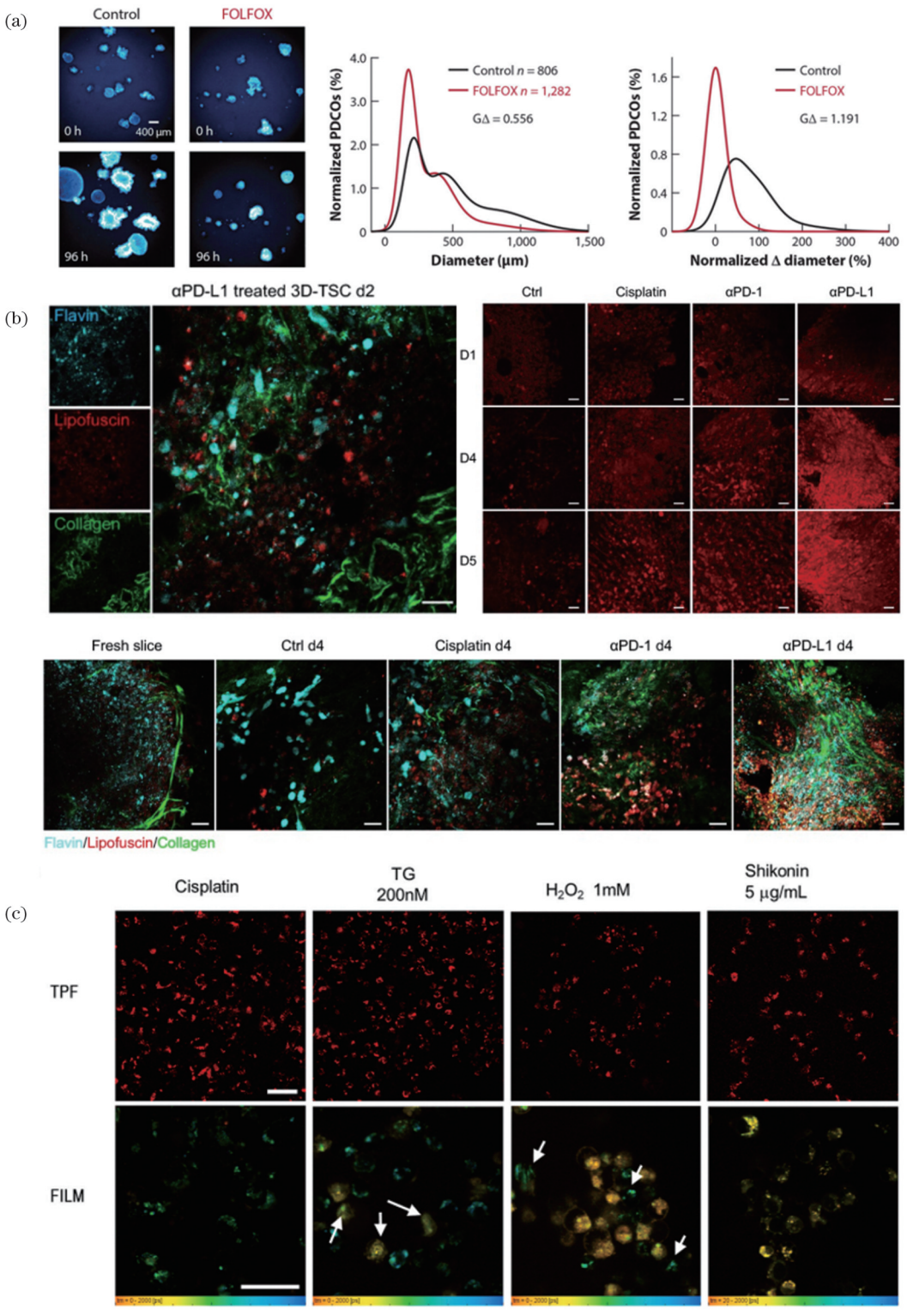

图 5 自发荧光显微成像揭示肿瘤细胞的药物干预反应。(a)基于来自 NAD(P)H 还原形式的自发荧光进行细胞和类器官水平的药物敏感性检测[94],比例尺为 400 μm;(b)双光子荧光显微镜对组织模型中胶原蛋白、脂褐素和黄素自发荧光的检测可以预测肿瘤对化疗和免疫治疗的反应[95],比例尺为 24 μm;(c)通过双光子荧光和荧光寿命成像(FLIM)获得应激诱导的脂褐素自体荧光寿命参数能够在单个细胞水平上区分细胞坏死与凋亡[96],比例尺为 50 μm

Fig. 5 Autofluorescence microscopy reveals drug intervention responses in tumor cells. (a) Detecting drug sensitivity at the cellular and organoid levels based on autofluorescence from the reduced form of NAD(P)H[94], with scale bar of 400 μm; (b) two-photon fluorescence microscopy for detecting collagen, lipofuscin, and flavin autofluorescence in tissue models can predict tumor responses to chemotherapy and immunotherapy[95], with scale bar of 24 μm; (c) obtaining lipofuscin autofluorescence lifetime parameter through two-photon fluorescence imaging and fluorescence lifetime imaging (FLIM) techniques can distinguish between apoptosis and necrosis in individual cell level[96], with scale bar of 50 μm

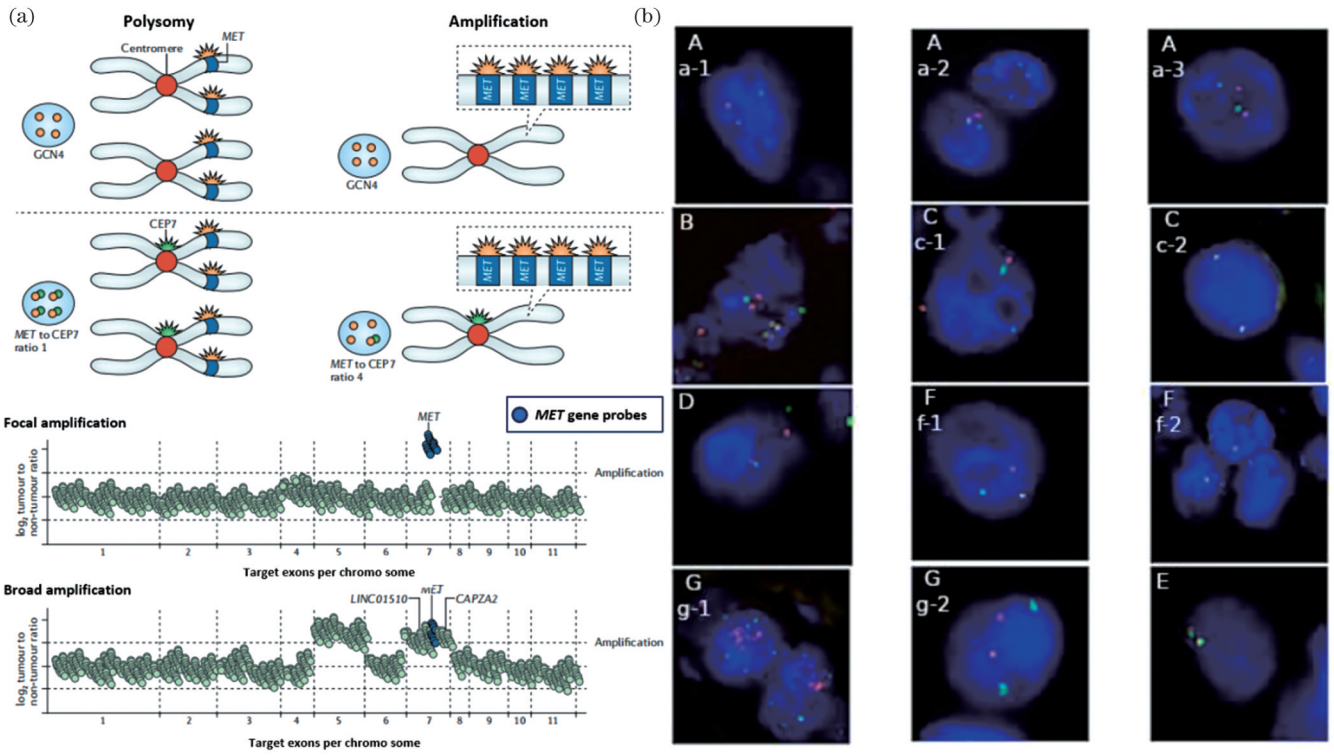

图 6 荧光原位杂交成像检测靶向治疗标志物及相关肿瘤分子特征。(a)致癌基因 MET 的扩增形式可通过荧光原位杂交技术进行区分,从而可以分析该基因扩增模式与肿瘤生物学行为的关系[102];(b)荧光原位杂交显微成像可对肺癌、胶质瘤和乳腺癌等多种肿瘤组织中的基因重排、融合、扩增和缺失等遗传异常进行检测和分析[103]

Fig. 6 Fluorescence *in situ* hybridization (FISH) imaging detects biomarkers for targeted therapy and related tumor molecular characteristics. (a) Amplification patterns of the oncogene MET can be distinguished using fluorescence *in situ* hybridization technology to analyze the relationship between this gene amplification pattern and tumor biological behavior[102]; (b) fluorescence *in situ* hybridization microscopy can detect and analyze genetic abnormalities such as rearrangements, fusions, amplifications, and deletions in various tumor tissues including lung cancer, gliomas, and breast cancer[103]

3.4 二次谐波(SHG)显微成像

二次谐波(SHG)显微成像近年来在肿瘤精准医疗领域的研究也有诸多进展。它利用激光在非中心对称结构(如胶原纤维)上散射产生的二次谐波信号进行显微成像,可在不需要对样本进行处理和染色的前提下,对组织样本进行成像并提供特定的成分信息。作为生物结构检测和耐久追踪标记的新工具,其在肿瘤微环境和肿瘤分级等的研究中受到了广泛关注。在二次谐波显微成像检测到的胶原纤维图像中可以观察到胶原纤维的排列方式和分布特点,胶原纤维在恶性样本中往往沿着单一方向高度对齐,这与肿瘤的侵袭性和预后有关。二次谐波显微成像可以辅助病理学家对肿瘤进行分级和分期,定量分析胶原纤维可以提高肿瘤分级的准确性,从而有助于医生作出更适宜的治疗方案[105]。

西奈山伊坎医学院的 Di Martino 团队[106],使用二次谐波显微成像技术分析了肿瘤组织的细胞外基质(ECM)特征,特别是肿瘤细胞休眠和增殖状态之间的 ECM 差异。该团队使用二次谐波成像技术比较了休眠和增殖肿瘤细胞周围的 ECM 结构,结果显示,与增殖肿瘤细胞相比,休眠肿瘤细胞周围的 ECM 主要由波浪状胶原纤维组成,并且胶原纤维的线性排列程度较低。他们通过测量胶原纤维的方向性发现休眠肿瘤中的胶原纤维方向性较低,而增殖肿瘤中胶原纤维的方向性较高,如图 7(a)所示。进而,该团队使用二次谐波成像技术分析了头颈部鳞状细胞癌(HNSCC)患者的肿瘤组织微阵列,结果显示,与淋巴结阳性患者相比,淋巴结阴性患者肿瘤组织中的 III 型胶原水平更高。这种 III 型胶原丰富的 ECM 微环境通过 DDR1 (discoidin domain receptor tyrosine kinase)和 STAT1 (signal transducer and activator of transcription 1)信号通路来维持肿瘤细胞的休眠状态。接着,该团队通过在体外和体内实验中操纵 III 型胶原水平,验证了其在肿瘤细胞休眠中的作用。他们发现:在体外实验中,增加 III 型胶原含量可以诱导肿瘤细胞进入休眠状态;而在体内实验中,使用 III 型胶原富集的生物工程支架可以减小局部复发的概率。基于这些发现,该团队提出了肿瘤细胞休眠和 ECM 的关联机制,为相关肿瘤进行检测和治疗提供了新的潜在靶点[106]。

约翰霍普金斯大学的 Zaver Bhujwalla 教授团队[107]使用二次谐波显微成像技术研究了前列腺癌转

移过程中细胞外基质(ECM)的功能和特征,并对人类前列腺癌异种移植物中Ⅰ型胶原(Col1)的纤维形态进行了表征。他们通过比较易于转移的原位肿瘤和转移能力较差的皮下肿瘤,观察到了原位肿瘤与皮下肿瘤在Col1纤维模式上的显著差异,并认为这可能与肿瘤微环境中的低氧状态有关,如图7(b)所示。该团队还使用二次谐波显微镜对人类前列腺癌组织微阵列进行了成像,以检测正常组织、癌旁组织、未发生转移的原发前列腺癌组织和已发生转移的原发前列腺癌组织中的Col1纤维形态,如图7(c)所示。与前述研究一致,恶性前列腺癌组织中的Col1纤维比正常组织的对齐程度和线性更高。该研究团队结合二次谐波成像结果和磁共振成像(MRI)衍生的宏分子运输参数发现,肿瘤中宏分子运输参数与Col1纤维的含量成正相关,强调了癌症相关成纤维细胞(CAFs)在促进肿瘤侵袭方面的作用以及在前列腺癌治疗中减少CAFs的重要性。这些发现提供了有关前列腺癌预后判断和治疗策略的新见解[107]。

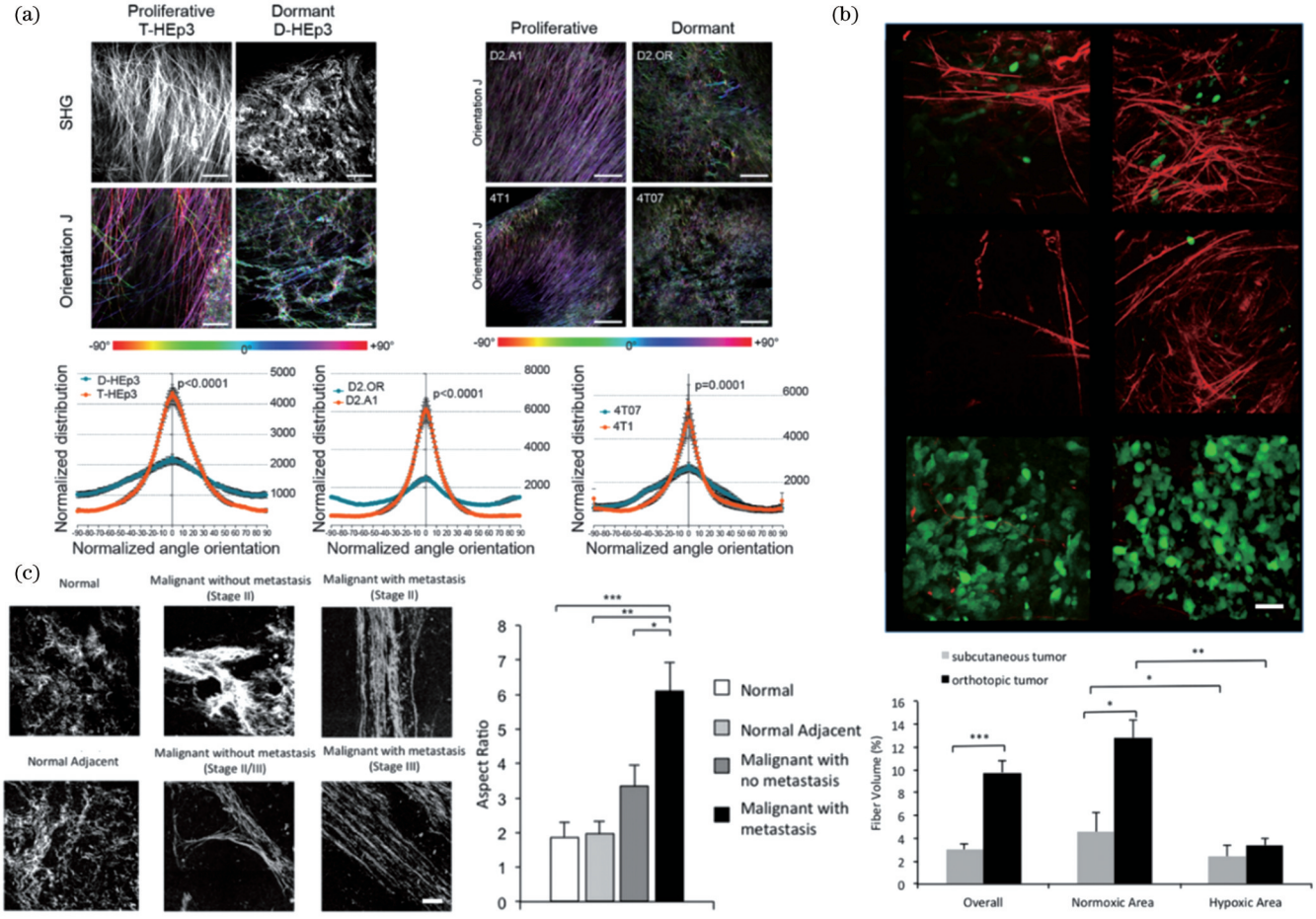

图7 二次谐波显微成像,可通过胶原纤维等细胞外基质特征研究肿瘤分期判定和转移性预测。(a)二次谐波显微成像显示,与增殖肿瘤细胞相比,休眠肿瘤细胞外基质胶原纤维线性排列程度低且方向性更高[106],比例尺为100 μm;(b)基于二次谐波显微图像可以发现易于转移的原位肿瘤中Ⅰ型胶原(Col1)的面积明显高于转移能力较差的皮下肿瘤,并且这种区分在肿瘤的常氧区域更为显著[107],比例尺为60 μm;(c)正常组织、正常邻近组织、未发生转移的恶性组织以及已发生转移的恶性组织的二次谐波图像显示,随着肿瘤恶性程度的增加,纤维的长宽比显著递增[107],比例尺为60 μm

Fig. 7 Second harmonic generation (SHG) microscopy reveals information about extracellular matrix components such as collagen to elucidate tumor staging and metastatic potential. (a) SHG microscopy images illustrate that, compared to proliferating tumor cells, dormant tumor cells have a lower degree of linear alignment and higher directionalality of extracellular matrix collagen fibers[106], scale bar: 100 μm; (b) SHG-based microscopy image reveals that *in situ* tumors with a propensity for metastasis have a significantly higher area of type I collagen (Col1) than subcutaneous tumors with less metastatic potential, and this distinction is more pronounced in the normoxic regions of the tumors[107], scale bar: 60 μm; (c) SHG images of normal tissue, adjacent normal tissue, malignant tissue without metastasis, and malignant tissue with metastasis show that as the malignancy of the tumor increases, the aspect ratio of the fibers increases significantly[107], scale bar: 60 μm

此外,康星大学的Eliceiri教授团队[108]使用二次谐波显微镜对乳腺癌、胰腺癌和结直肠癌等肿瘤组织的胶原纤维进行了分析,探讨了胶原纤维组织是如何影响肿瘤微环境的,包括肿瘤细胞的侵袭和免疫细胞的

迁移。Bian教授团队[109]利用二次谐波显微成像技术研究了胃癌微环境中胶原纤维的变化及其与预后的关系，结果发现胶原纤维的长宽比可以作为判断胃癌预后的有力指标。威斯康星大学的Best等[110]利用二次谐波显微成像技术研究了肾细胞癌(RCC)中胶原纤维组织的排列，并探讨了其与肿瘤分级的相关性。结果显示，胶原纤维的密度和排列在不同分级的RCC中表现出了显著差异，这有助于提高肾肿瘤分级判定的准确率。另外，二次谐波还可与三次谐波(THG)及多光子激发荧光(2PEF/3PEF)等成像方案结合，提供更为丰富的肿瘤组织成像信息。例如，结合二次谐波与三次谐波成像可以通过脂质膜状结构和DNA聚集形成的光学界面，实现肿瘤的可视化。该方法不仅在脑胶质瘤组织中获得了与金标准(H&E病理分析)一致的肿瘤病理图像，还获得了细胞增生、核多形性与血管增殖等信息[111]。

3.5 相干拉曼散射(CRS)显微成像

随着光学技术的不断发展，以多重免疫荧光和荧光原位杂交为代表的显微成像技术成为现代肿瘤医学研究的重要手段。然而，基于荧光的显微技术存在一定局限性，例如：荧光标记分子的引入会干扰细胞的正常生化过程；荧光信号需要高能激发光激发电子使之跃迁才可产生，样本易受到激发光的伤害；荧光基团存在的光漂白现象限制了样本的长时间观察；很多重要的研究目标物，如细胞内的糖类和脂类小分子，难以或无法被荧光基团标记。自发拉曼散射不需要对样品进行任何化学或荧光标记，是一种无干扰的成像方法，适用于活体肿瘤细胞和组织的成像分析，能够实现高空间分辨率成像并能提供分子振动的指纹信息，可以区分不同的化学键和分子结构，在分子识别和分析方面具有非常大的价值[112]。但自发拉曼散射成像也有其自身的缺陷，如灵敏度较低且成像速度受限，较低的通量限制了其在肿瘤精准诊疗领域的应用。

与自发拉曼散射一样，相干拉曼散射(CRS)仍将分子键振动作为成像的基础，但它可以通过非线性光学效应使拉曼散射信号显著增强，从而提高成像速度和检测灵敏度。相干拉曼散射主要包括相干反斯托克斯拉曼散射(CARS)与受激拉曼散射(SRS)显微成像技术。CARS成像技术于1982年诞生于美国海军实验室[113]，然而由于CARS过程中的电子跃迁可绕过分子键振动直接通过虚能级产生，因而CARS信号存在非共振背景的干扰。为了解决此问题，哈佛大学的谢晓亮课题组在2008年推出了SRS技术[114]。SRS是一种基于受激过程的技术。在该技术中，两束频率差与特定分子键振动频率匹配的激光(泵浦光和斯托克斯光)通过受激激发实现拉曼信号的放大，同时发生激发光子与分子键振动之间的共振能量交换，使泵浦光束和斯托克斯光束强度发生仅依赖特定分子键振动的变化，分别是受激拉曼增益(SRG)和受激拉曼损耗(SRL)，然后对SRG/SRL进行定量检测，实现成像。该技术具有严格的分子键共振特征，不再受非共振背景的干扰，因而不但在光谱上与自发拉曼一致，并且可以通过分子能级共振效应将拉曼成像信号强度和成像速度提高10^4～10^6倍，在非侵入、无损的前提下提供高灵敏度高时空分辨的生物样本化学信息成像，在肿瘤精准医疗研究领域具有巨大潜力。

2020年，美国加州理工学院的Wei团队[115]利用SRS显微成像技术研究了转移性黑色素瘤细胞的代谢特征。他们使用SRS技术对黑色素瘤单细胞的代谢物进行了成像和空间映射，比较了不同细胞系脂代谢强度的差异，并分析了这些差异与脂肪酸合成相关基因的关系，如图8(a)所示。他们发现：脂肪酸合成途径可作为黑色素瘤药物脆弱性的识别指征；脱分化间充质细胞中脂质单不饱和度与BRAF抑制的固有抵抗有关。他们将SRS成像结果与脂质组学和转录组学结合起来进行分析，提出了基于脂质代谢调控的潜在治疗途径。SRS成像技术可揭示单细胞的代谢异质性，这对于开发针对特定细胞亚群的个性化治疗方案具有重要意义。该工作展现了SRS显微成像技术在肿瘤精准医疗研究中的潜力，特别是在识别和验证药物靶点、理解肿瘤细胞代谢异质性以及实时观察药物响应等方面具有巨大潜力。

通过对耐药肿瘤细胞代谢重编程表型进行研究，波士顿大学的程继新教授课题组利用SRS显微成像技术发现了铂类耐药细胞在代谢上的显著变化，这些变化包括脂肪酸(FA)摄取的增加以及葡萄糖摄取和糖源性脂质生成的减少。这一发现表明癌细胞从葡萄糖依赖的合成和能量代谢转变为脂肪酸依赖。该课题组提出了一个“代谢指数”，即葡萄糖衍生和脂肪酸摄取的比值(如图8(b)所示)。该指数与卵巢癌细胞对铂类药物的耐药水平呈线性相关，展现了SRS成像用于快速检测铂类药物耐药的能力[116]。另外，该课题组利用SRS显微成像技术研究了卵巢癌干细胞(CSCs)的代谢特征，结果显示：与非卵巢癌干细胞相比，卵巢癌干细胞具有显著增加的不饱和脂肪酸水平。这表明不饱和脂肪酸可能是卵巢癌干细胞的代谢标志物，并提示脂质重塑是卵巢癌干细胞的一个特异性治疗靶点，为开发新的治疗策略提供了理论基础[117]。从代谢变化监控的角度，Bardhan教授课题组[118]利用拉曼显微成像监测了KRAS突变的结直肠癌(CRC)HCT116细胞在药物作用下的关键代谢物变化，并将其作为早期预测治疗反应的指标。研究发现，HCT116细胞对西妥昔单抗(CTX)这种一线治疗药物具有抵抗性，但预先用奥沙利铂(OX)进行细胞敏化可以克服这种抗性。该研究指出脂质和氨基酸的代谢指征可作为

预测肿瘤细胞对治疗抵抗程度的指标，基于拉曼显微成像的代谢检测有能力预测临床肿瘤治疗的反应和预后。

基于临床对肿瘤脱落细胞高通量检测和化疗治疗效果评估的迫切需求，北京航空航天大学的岳蜀华教授团队[119]利用SRS显微成像技术对腹腔灌洗脱落细胞进行了成像分析，以提高胃癌（GC）腹膜转移（PM）的检测准确率和速度。他们将SRS图像与深度学习算法结合，开发出了一种结合K-means和主成分分析（PCA）的K-PCA算法，用其进行细胞分型。同时，他们从腹膜灌洗液中提取单个脱落细胞的形态和组分特征，以更准确地区分腹膜转移阳性和阴性标本，显著提高了检测的敏感度、特异度及速度。

此外，凭借SRS系统兼具图像与光谱信息采集的优势，麻省理工-哈佛博德研究所的Regev教授团队[120]通过整合高光谱SRS显微图像和多模态数据，推断出了活细胞中的基因表达谱。在研究中，他们将空间分辨单分子RNA-FISH（smFISH）数据作为锚点，将scRNA-seq图谱与配对的空间高光谱拉曼图像结合起来，使用机器学习模型从单细胞水平高光谱显微成像中推断出了基因表达谱，如图8（c）所示。该工作展示了SRS检测技术在连接肿瘤精准医疗基因型和表型研究范式方面的能力。

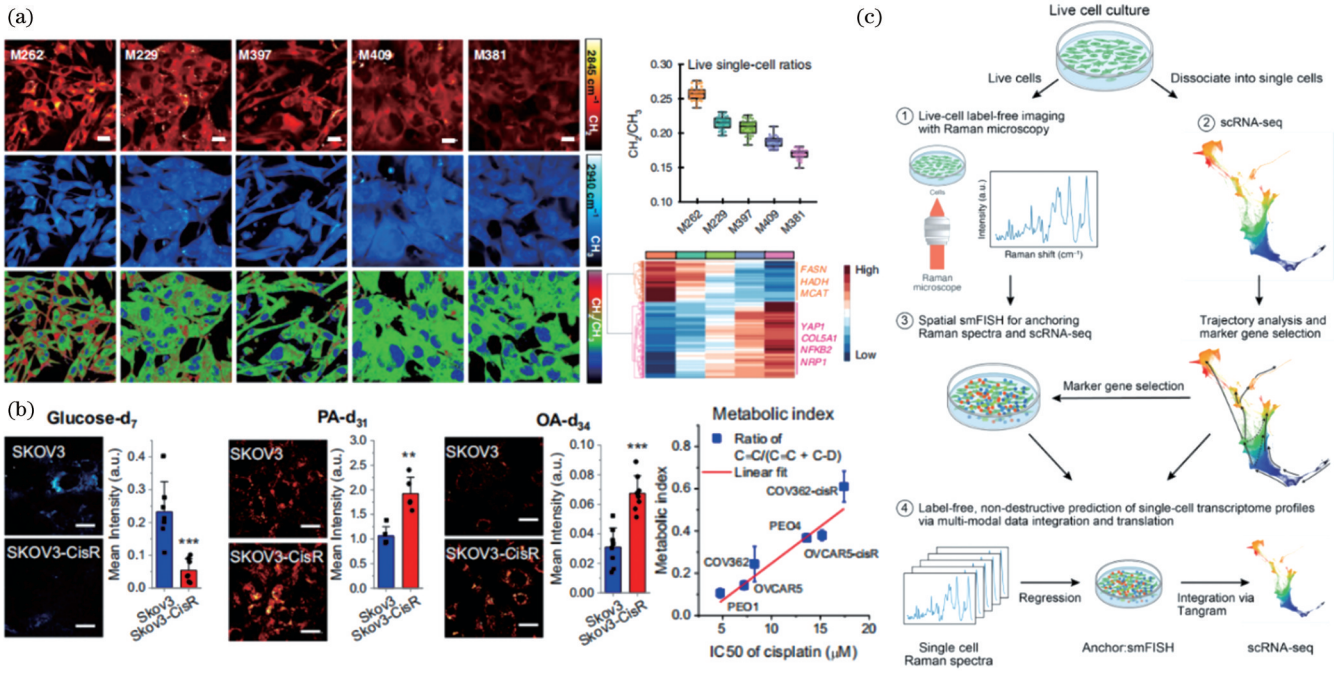

图8 SRS成像为肿瘤精准医疗提供了更深入的洞察。（a）基于SRS的活细胞成像构建细胞表型与基因型关系，以解释黑色素瘤细胞代谢重编程机理，揭示代谢干预治疗的潜在靶点[115]，比例尺：20 μm；（b）SRS观测到顺铂耐药细胞从葡萄糖向脂肪酸依赖的代谢变化，基于对SRS图像的定量分析得出的代谢指数可用于肿瘤耐药预测[116]，比例尺：20 μm；（c）Raman2RNA（R2R）的工作流程，包括细胞培养、细胞分子振动能级检测、单分子RNA荧光原位杂交（smFISH）成像、并行培养细胞的单细胞RNA测序（scRNA-seq），以及通过机器学习和多模态数据整合从拉曼光谱中预测单细胞RNA-seq表达谱[120]

Fig. 8 Stimulated Raman scattering (SRS) imaging provides deeper insights for precision medicine in cancer. (a) SRS-based live cell imaging elucidates the relationship between cell phenotype and genotype, explaining the metabolic reprogramming mechanisms of melanoma cells, revealing potential targets for metabolic intervention therapy[115], scale bar: 20 μm; (b) SRS observes metabolic shifts from glucose to fatty acid dependence in cisplatin-resistant cells, and metabolic index derived from quantitative analysis of SRS images can be used for tumor resistance prediction[116], scale bar: 20 μm; (c) the workflow of Raman2RNA (R2R) encompasses cell culturing, molecular vibrational energy level detection of cells, single-molecule RNA fluorescence *in situ* hybridization (smFISH) imaging, parallel single-cell RNA sequencing (scRNA-seq) of cultured cells, and the prediction of single-cell RNA-seq expression profiles from Raman spectra through machine learning and multi-modal data integration[120]

近10年来，SRS显微技术高速发展，除上述研究外，该技术在肿瘤精准医疗领域还有诸多进展。研究人员基于SRS技术对新鲜肿瘤组织进行快速成像，通过脂质和蛋白质双通道成像，得到了与病理学金标准H&E图像高度一致的双色SRS图像[121-122]。类似地，SRS技术基于肿瘤组织与正常组织的成分差异可对肿瘤边缘进行定位，并可对脑胶质瘤切除等高精度手术进行实时精准指引[123]。岳蜀华等[124]发挥SRS显微成像和成分分析的特点，对前列腺肿瘤组织进行了单细胞脂质成分定量分析，推动了前列腺癌诊断及新型干预治疗靶点的发现。另外，通过小分子标记方式，SRS成像可以识别新合成生物分子从而观测代谢

过程。如，闵玮课题组[125]与黄岩谊课题组[126]利用氘代和炔基等拉曼标记物研究了肿瘤等生物样本中脂质[127]、蛋白质[128-130]和糖类[131-133]的代谢特征，为从微观示踪角度研究代谢组学提供了新工具。应该指出的是，拉曼探针通过特定分子键或分子共振特征提供成像信号，有效避免了大分子染料对生物体的干扰，因而基于分子键标定的SRS系统可同时对水、脂和糖等代谢分子进行高时空分辨和高灵敏度成像。同时，拉曼探针凭借窄峰宽可以轻易实现超多重标定成像，避免了多重免疫荧光成像的反复洗脱过程，为肿瘤精准医疗研究提供了更高通量和更高内涵的研究工具。

3.6 其他光学显微成像技术在肿瘤精准医疗领域的研究进展

除了上述技术外，近年来在中红外(MIR)共振和光热显微成像以及瞬态吸收显微成像(TAM)等方向，也有诸多推进肿瘤精准医疗实践的新进展。

在中红外(MIR)共振显微成像方面，哥伦比亚大学的Min教授团队[134]提出了一种新的被称为振动绘画(VIBRANT)的高内涵光谱成像和分析方法。研究者结合中红外振动成像、多重振动探针和创新数据分析方法，将振动光谱与成像技术相结合，在单细胞水平上监测了肿瘤细胞对药物干预后的生物化学反应。该技术使用三种红外活性振动探针来测量肿瘤细胞的基本代谢活动，即利用13C-氨基酸(13C-AA)和叠氮棕榈酸(叠氮PA)反映蛋白质合成和饱和脂肪酸代谢，同时利用氘化油酸(d34OA)反映不饱和脂肪酸代谢，结合机器学习分类器在单细胞水平上精准预测药物的作用机制(MoA)并最小化批次效应。VIBRANT技术能够在单细胞水平上提供关于药物反应的详细信息，有助于药物发现和个性化医疗策略的制定。

中红外光热(MIP)成像利用中红外光激发生物分子的振动吸收，同时利用可见光束探测由热透镜效应引起的光束扰动，能达到亚微米级的空间分辨率，超越了红外显微镜的衍射极限，可对活细胞和生物体进行无标记三维化学成像。波士顿大学的程继新教授团队[135]使用中红外光热成像技术对PC-3前列腺癌细胞中的脂滴进行了深度成像。通过调整中红外激光的波数至C═O键的振动峰(1750 cm^{-1})，他们成功观察到了脂滴在细胞内的3D分布，如图9(a)所示。同时，他们还利用MIP技术对MIA PaCa-2胰腺癌细胞中JZL184药物分子的吸收进行了观测，通过多光谱MIP成像定位了药物分子在细胞内的分布，如图9(b)所示，这对于研究药物的作用机制和优化药物治疗策略具有重要价值。该课题组后续提出了名为“nitrile chameleons”的新型酶切探针，这些探针通过特定酶切反应产生可被MIP成像检测的信号。通过使用特定的nitrile chameleon酶切探针，研究者能在细胞内精确测量与探针相互作用的酶的活性，并观察它们在细胞内的异质分布。程继新教授团队[135]使用MIP技术实时监测了经化疗药(多柔比星)处理的SJSA-1骨肉瘤细胞中磷酸酶和半胱天冬酶-3/7的活性(如图9(c)所示)，这些酶在细胞存活和凋亡过程中起关键作用[136]。这些研究证明了MIP成像技术可应用于药物作用分析，同时通过映射酶的活性变化有助于发现和优化针对特定酶的潜在药物。

另外，Liu等[137]利用瞬态吸收显微成像技术和金纳米粒子(AuNPs)探针，评估了人类表皮生长因子受体2(Her2)mRNA在癌细胞和乳腺癌组织中的表达。基于瞬态吸收显微成像技术和SRS成像的结合，Liu等在单细胞水平上对Her2 mRNA的表达进行了定量测量。如图9(d)所示，MCF-7细胞系中Her2 mRNA的表达水平较低，而SK-BR-3细胞系中Her2 mRNA过度表达。为了验证瞬态吸收显微成像策略的有效性，与Aviv Regev教授团队利用荧光原位杂交成像数据作为锚定[120]的思路类似，Liu等[137]将瞬态吸收显微成像结果与荧光原位杂交数据进行比较，证实了瞬态吸收显微成像技术在单细胞水平上对Her2 mRNA表达进行定量分析的准确性[137]。另外，东南大学的崔一平教授团队[138]利用表面增强拉曼散射(SERS)技术，基于由金纳米粒子、拉曼报告分子(DTNB)以及DNA修饰物组成的SERS纳米探针，通过DNA功能化水凝胶的新型外泌体检测方法，实现了SERS纳米探针光学信号的放大，通过监测SERS信号的变化定量且灵敏地检测了肿瘤源性外泌体，为实体肿瘤的早期诊断提供了新路径。

4 结束语

肿瘤精准医疗的核心是为患者提供个性化的治疗方案，以获得更好的治疗效果和预后。尽管基因测序技术(如NGS)在肿瘤精准医疗方面取得了显著进展，但由于肿瘤的获得性耐药、人们对基因突变理解不全面，以及基因突变和肿瘤表型关联的复杂性，其在指导临床治疗方面仍存在很大局限性。此外，基于肿瘤细胞活性和增殖的传统表型功能检测方法，无法提供关于肿瘤组织微环境、分子特征和代谢组学等方面的深入见解，难以建立与测序结果的机制关联。同时，该方法所需样本量较大且需要较长时间的模型构建和培养，导致其对亲代肿瘤的表征一致性差、检测周期长且成本高。

光学显微成像能够基于有限样本进行高通量检测，具备对肿瘤样本微环境、基因组、蛋白组与代谢分子特征等诸多要素的深度检测和分析能力，已成为肿瘤精准医疗研究的重要手段。多重免疫荧光显微成像能够对肿瘤组织中不同类型细胞的构成和比例、细胞相互作用、特定蛋白表达和含量进行成像和分析；自发荧光显微成像技术提供了一种可以评估药物反

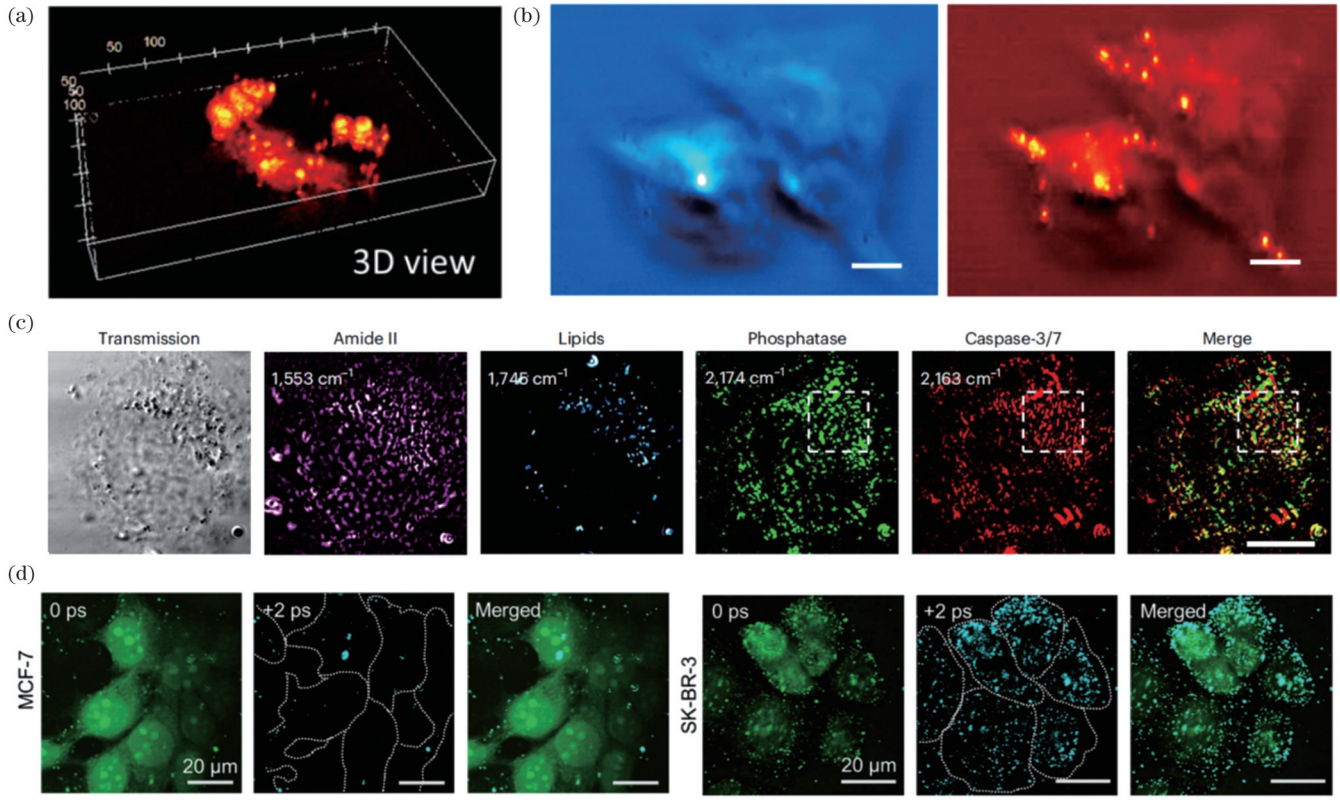

图 9 中红外(MIR)光热显微成像和瞬态吸收(TA)显微技术可提供亚细胞生化分子图像。(a)PC-3 前列腺癌细胞的中红外光热成像三维视图,细胞体内的单个脂滴清晰可见[135];(b)对经 JZL184 处理的 MIA PaCa-2 胰腺癌细胞进行 MIP 成像,通过多变量曲线分辨(MCR)分析得出了可定量显示细胞内药物和脂质含量分布的图像[135],比例尺:20 μm;(c)多色中红外光热成像可视化经 Dox(多柔比星)和腈标记酶活性探针预处理的 SJSA-1 细胞中磷酸酶和半胱天冬酶-3/7 活性分布的实验结果[136](从左往右依次为明场像以及蛋白、脂滴、磷酸酶、半胱天冬酶-3/7 图像和酶活性融合图像),比例尺:40 μm;(d)瞬态吸收显微技术通过对与 Her2 mRNA 结合的 AuNPs 探针成像,展示了 MCF-7 和 SK-BR-3 乳腺癌细胞中 Her2 mRNA 的表达水平和定位模式[137],比例尺:20 μm

Fig. 9 Mid-infrared (MIR) photothermal microscopy and transient absorption (TA) microscopy techniques provide subcellular biochemical molecular imaging. (a) A three-dimensional view of mid-infrared photothermal imaging of PC-3 prostate cancer cells, clearly showing individual lipid droplets within the cells[135]; (b) MIP imaging results of MIA PaCa-2 pancreatic cancer cells treated with JZL184, with images quantitatively displaying the distribution of intracellular drug and lipid content derived from multivariate curve resolution (MCR) analysis[135], scale bar: 20 μm; (c) multicolor mid-infrared photothermal imaging of SJSA-1 cells pretreated with Dox (doxorubicin) and a cyanine-labeled enzyme activity probe, visualizing the distribution of phosphatase and caspase-3/7 activity (from left to right are brightfield, protein, lipid droplets, phosphatase, caspase-3/7, and the merged enzyme activity images)[136], scale bar: 40 μm; (d) transient absorption microscopy imaging the AuNPs (gold nanoparticles) probe bound to Her2 mRNA, demonstrating the expression levels and localization patterns of Her2 mRNA in MCF-7 and SK-BR-3 breast cancer cells[137], scale bar: 20 μm

应和肿瘤异质性的直观、非侵入性方法;荧光原位杂交显微成像利用荧光偶联的 DNA 片段来检测和分析感兴趣的基因组区域,有助于识别肿瘤的分子特征;二次谐波显微成像通过对肿瘤微环境中胶原的含量和形态等数据进行分析,提高了肿瘤分级和分期的准确性,并为诊断和治疗提供了新靶点。SRS 成像技术凭借其高灵敏度、高时空分辨率和非侵入的特点,能够揭示肿瘤样本的单细胞化学图谱和代谢特征,可以监测药物响应并预测肿瘤耐药性,同时助力肿瘤快速病理和新治疗手段的探索。其他的光学显微成像技术,如中红外共振或光热显微成像以及瞬态吸收显微成像技术,亦是研究肿瘤药物作用和早期诊断等的有效工具。

综上,光学显微成像技术可在肿瘤微环境分析、肿瘤细胞代谢特征、基因到蛋白通路以及药物敏感性评估等研究领域提供新的研究策略和临床工具(如表 1 所示),在肿瘤研究和诊疗中发挥愈加重要的作用。展望未来,光学显微成像技术和设备的进一步发展和优化将克服设备成本高和图像分析复杂等局限,为肿瘤诊疗在个性化、精准性以及效率方面带来更大突破,成为理解肿瘤基因型到表型的桥梁和开启肿瘤精准医疗的钥匙。

表 1 相关光学显微成像技术在肿瘤精准医疗领域的应用场景与技术对比

Table 1 Application scenarios and technical comparisons of relevant optical microscopy techniques in the field of precision oncology

Technique	Application scenario	Resolution	Imaging speed	Sensitivity	Technical advantage	Application limitation
Multiplex immunofluorescence (mIF)	1) Tumor microenvironment analysis 2) Cell interaction immunotherapy evaluation	Subcellular level (<1 μm)	s–min	High (nmol/L)	Simultaneously detect multiple biomarkers, providing rich spatial information	Requires specific fluorescent probes, potential for fluorescence crosstalk, optical properties of the sample are requirement
Autofluorescence (AF)	1) Drug response assessment 2) Tumor heterogeneity research 3) Metabolic activity monitoring	Subcellular level (1–5 μm)	ms–s	Moderate (μmol/L)	No need for exogenous labeling, reduces interference to the sample	Limited by the intrinsic fluorescence properties of the sample, requires complex data processing to differentiate between different fluorescence signals
Fluorescence *in situ* hybridization (FISH)	1) Gene copy number analysis 2) Genetic abnormality detection 3) Tumor molecular typing	Subcellular level (<1 μm)	s–min	High (nmol/L)	Provides precise information on gene expression and localization	Requires specific probe design, time-consuming hybridization process, high demands on sample preservation state
Second harmonic generation (SHG)	1) Extracellular matrix analysis 2) Tumor grading 3) Invasion and metastasis research	Submicron scale (<100 nm)	ms–s	High (nmol/L)	Provides non-invasive high-resolution imaging, no need for exogenous markers	Limited by non-centrosymmetric structures such as collagen, high optical transparency of the sample is required
Coherent Raman scattering (CRS)	1) Tumor metabolite imaging 2) Drug target identification 3) Cellular pathology detection	Subcellular level (<1 μm)	ms–s	High (pmol/L)	Provides molecular-level chemical information, no need for labeling	Limited by the Raman activity of the sample and imaging depth, requires complex data processing
Mid-infrared photothermal (MIR)	1) Drug PK/PD research 2) Metabolic spatial distribution 3) 3D imaging of tumor samples	Submicron scale (<100 nm)	ms–s	High (nmol/L)	Capable of performing label-free 3D imaging, friendly to live cells and tissues	Limited penetration ability, and requires optimization of light sources and detectors
Transient absorption (TA)	1) mRNA expression and localization 2) Gene expression regulation 3) Drug mechanism of action	Subcellular level (<1 μm)	ms–s	High (nmol/L)	Capable of rapid dynamic imaging, sensitive to high temporal resolution biological processes	Requires specific sample absorption characteristics, optimization of laser pulse and detection technology needed

参 考 文 献

[1] Lai Y H, Lin S Y, Wu Y S, et al. AC-93253 iodide, a novel Src inhibitor, suppresses NSCLC progression by modulating multiple Src-related signaling pathways[J]. Journal of Hematology & Oncology, 2017, 10(1): 172.

[2] Lai Y X, Wei X R, Lin S H, et al. Current status and perspectives of patient-derived xenograft models in cancer research[J]. Journal of Hematology & Oncology, 2017, 10(1): 106.

[3] Meng S J, Zhou H C, Feng Z Y, et al. CircRNA: functions and properties of a novel potential biomarker for cancer[J]. Molecular Cancer, 2017, 16(1): 94.

[4] Li A C, Zhang T B, Zheng M, et al. Exosomal proteins as potential markers of tumor diagnosis[J]. Journal of Hematology & Oncology, 2017, 10(1): 175.

[5] Viardot A, Bargou R. Bispecific antibodies in haematological malignancies[J]. Cancer Treatment Reviews, 2018, 65: 87-95.

[6] Yu S N, Liu Q, Han X W, et al. Development and clinical application of anti-HER2 monoclonal and bispecific antibodies for cancer treatment[J]. Experimental Hematology & Oncology, 2017, 6: 31.

[7] Yu S N, Li A P, Liu Q, et al. Recent advances of bispecific antibodies in solid tumors[J]. Journal of Hematology & Oncology, 2017, 10(1): 155.

[8] Yi M, Jiao D C, Xu H X, et al. Biomarkers for predicting efficacy

of PD-1/PD-L1 inhibitors[J]. Molecular Cancer, 2018, 17(1): 129.
[9] Wei G Q, Ding L J, Wang J S, et al. Advances of CD19-directed chimeric antigen receptor-modified T cells in refractory/relapsed acute lymphoblastic leukemia[J]. Experimental Hematology & Oncology, 2017, 6: 10.
[10] Xu H X, Yu S N, Liu Q, et al. Recent advances of highly selective CDK4/6 inhibitors in breast cancer[J]. Journal of Hematology & Oncology, 2017, 10(1): 97.
[11] Pang Y Y, Hou X Y, Yang C S, et al. Advances on chimeric antigen receptor-modified T-cell therapy for oncotherapy[J]. Molecular Cancer, 2018, 17(1): 91.
[12] Liu B S, Song Y P, Liu D L. Recent development in clinical applications of PD-1 and PD-L1 antibodies for cancer immunotherapy[J]. Journal of Hematology & Oncology, 2017, 10(1): 174.
[13] Sicklick J K, Kato S, Okamura R, et al. Molecular profiling of cancer patients enables personalized combination therapy: the I-PREDICT study[J]. Nature Medicine, 2019, 25(5): 744-750.
[14] Rodon J, Soria J C, Berger R, et al. Genomic and transcriptomic profiling expands precision cancer medicine: the WINTHER trial [J]. Nature Medicine, 2019, 25(5): 751-758.
[15] Le Tourneau C, Borcoman E, Kamal M. Molecular profiling in precision medicine oncology[J]. Nature Medicine, 2019, 25(5): 711-712.
[16] International Human Genome Sequencing Consortium. Finishing the euchromatic sequence of the human genome[J]. Nature, 2004, 431(7011): 931-945.
[17] Margulies M, Egholm M, Altman W E, et al. Genome sequencing in microfabricated high-density picolitre reactors[J]. Nature, 2005, 437(7057): 376-380.
[18] Shendure J, Porreca G J, Reppas N B, et al. Accurate multiplex polony sequencing of an evolved bacterial genome[J]. Science, 2005, 309(5741): 1728-1732.
[19] Roberts K G, Morin R D, Zhang J H, et al. Genetic alterations activating kinase and cytokine receptor signaling in high-risk acute lymphoblastic leukemia[J]. Cancer Cell, 2012, 22(2): 153-166.
[20] Stacey S N, Sulem P, Jonasdottir A, et al. A germline variant in the TP53 polyadenylation signal confers cancer susceptibility[J]. Nature Genetics, 2011, 43(11): 1098-1103.
[21] Bass A J, Lawrence M S, Brace L E, et al. Genomic sequencing of colorectal adenocarcinomas identifies a recurrent VTI1A-TCF7L2 fusion[J]. Nature Genetics, 2011, 43(10): 964-968.
[22] Fujimoto A, Totoki Y, Abe T, et al. Whole-genome sequencing of liver cancers identifies etiological influences on mutation patterns and recurrent mutations in chromatin regulators[J]. Nature Genetics, 2012, 44(7): 760-764.
[23] Berger M F, Hodis E, Heffernan T P, et al. Melanoma genome sequencing reveals frequent PREX2 mutations[J]. Nature, 2012, 485(7399): 502-506.
[24] Cheung N K, Zhang J, Lu C, et al. St. Jude Children's Research Hospital–Washington University Pediatric Cancer Genome Project. Association of age at diagnosis and genetic mutations in patients with neuroblastoma [J]. JAMA, 2012, 307: 1062-1071.
[25] Rafnar T, Gudbjartsson D F, Sulem P, et al. Mutations in BRIP1 confer high risk of ovarian cancer[J]. Nature Genetics, 2011, 43(11): 1104-1107.
[26] Roychowdhury S, Iyer M K, Robinson D R, et al. Personalized oncology through integrative high-throughput sequencing: a pilot study[J]. Science Translational Medicine, 2011, 3(111): 111ra121.
[27] Guan Y F, Li G R, Wang R J, et al. Application of next-generation sequencing in clinical oncology to advance personalized treatment of cancer[J]. Chinese Journal of Cancer, 2012, 31(10): 463-470.
[28] Hopp K, Heyer C M, Hommerding C J, et al. B9D1 is revealed as a novel Meckel syndrome (MKS) gene by targeted exon-enriched next-generation sequencing and deletion analysis[J]. Human Molecular Genetics, 2011, 20(13): 2524-2534.
[29] Jones M A, Bhide S, Chin E, et al. Targeted polymerase chain reaction-based enrichment and next generation sequencing for diagnostic testing of congenital disorders of glycosylation[J]. Genetics in Medicine, 2011, 13(11): 921-932.
[30] Hollants S, Redeker E J W, Matthijs G. Microfluidic amplification as a tool for massive parallel sequencing of the familial hypercholesterolemia genes[J]. Clinical Chemistry, 2012, 58(4): 717-724.
[31] Wu C H, Fallini C, Ticozzi N, et al. Mutations in the profilin 1 gene cause familial amyotrophic lateral sclerosis[J]. Nature, 2012, 488(7412): 499-503.
[32] Veltman J A, Brunner H G. *De novo* mutations in human genetic disease[J]. Nature Reviews Genetics, 2012, 13(8): 565-575.
[33] Yan X J, Xu J, Gu Z H, et al. Exome sequencing identifies somatic mutations of DNA methyltransferase gene DNMT3A in acute monocytic leukemia[J]. Nature Genetics, 2011, 43(4): 309-315.
[34] Banerji S, Cibulskis K, Rangel-Escareno C, et al. Sequence analysis of mutations and translocations across breast cancer subtypes[J]. Nature, 2012, 486(7403): 405-409.
[35] Agrawal N, Frederick M J, Pickering C R, et al. Exome sequencing of head and neck squamous cell carcinoma reveals inactivating mutations in *NOTCH1*[J]. Science, 2011, 333(6046): 1154-1157.
[36] Quesada V, Conde L, Villamor N, et al. Exome sequencing identifies recurrent mutations of the splicing factor SF3B1 gene in chronic lymphocytic leukemia[J]. Nature Genetics, 2011, 44(1): 47-52.
[37] Xiong D H, Li G M, Li K Z, et al. Exome sequencing identifies MXRA5 as a novel cancer gene frequently mutated in non-small cell lung carcinoma from Chinese patients[J]. Carcinogenesis, 2012, 33(9): 1797-1805.
[38] Liu P Y, Morrison C, Wang L, et al. Identification of somatic mutations in non-small cell lung carcinomas using whole-exome sequencing[J]. Carcinogenesis, 2012, 33(7): 1270-1276.
[39] Krauthammer M, Kong Y, Ha B H, et al. Exome sequencing identifies recurrent somatic RAC1 mutations in melanoma[J]. Nature Genetics, 2012, 44(9): 1006-1014.
[40] Wei X M, Walia V, Lin J C, et al. Exome sequencing identifies GRIN2A as frequently mutated in melanoma[J]. Nature Genetics, 2011, 43(5): 442-446.
[41] Barbieri C E, Baca S C, Lawrence M S, et al. Exome sequencing identifies recurrent SPOP, FOXA1 and MED12 mutations in prostate cancer[J]. Nature Genetics, 2012, 44(6): 685-689.
[42] Zang Z J, Cutcutache I, Poon S L, et al. Exome sequencing of gastric adenocarcinoma identifies recurrent somatic mutations in cell adhesion and chromatin remodeling genes[J]. Nature Genetics, 2012, 44(5): 570-574.
[43] Yohe S, Thyagarajan B. Review of clinical next-generation sequencing[J]. Archives of Pathology & Laboratory Medicine, 2017, 141(11): 1544-1557.
[44] Muzzey D, Evans E A, Lieber C. Understanding the basics of NGS: from mechanism to variant calling[J]. Current Genetic Medicine Reports, 2015, 3(4): 158-165.
[45] Ponting C P. The functional repertoires of metazoan genomes[J]. Nature Reviews Genetics, 2008, 9(9): 689-698.
[46] Keren H, Lev-Maor G, Ast G. Alternative splicing and evolution: diversification, exon definition and function[J]. Nature Reviews Genetics, 2010, 11(5): 345-355.
[47] Akiva P, Toporik A, Edelheit S, et al. Transcription-mediated gene fusion in the human genome[J]. Genome Research, 2006, 16(1): 30-36.
[48] Katayama S, Tomaru Y, Kasukawa T, et al. Antisense transcription in the mammalian transcriptome[J]. Science, 2005, 309(5740): 1564-1566.
[49] Gott J M, Emeson R B. Functions and mechanisms of RNA editing [J]. Annual Review of Genetics, 2000, 34: 499-531.

[50] Maher C A, Kumar-Sinha C, Cao X H, et al. Transcriptome sequencing to detect gene fusions in cancer[J]. Nature, 2009, 458(7234): 97-101.

[51] Maher C A, Palanisamy N, Brenner J C, et al. Chimeric transcript discovery by paired-end transcriptome sequencing[J]. Proceedings of the National Academy of Sciences of the United States of America, 2009, 106(30): 12353-12358.

[52] Palanisamy N, Ateeq B, Kalyana-Sundaram S, et al. Rearrangements of the RAF kinase pathway in prostate cancer, gastric cancer and melanoma[J]. Nature Medicine, 2010, 16(7): 793-798.

[53] Pflueger D, Terry S, Sboner A, et al. Discovery of non-ETS gene fusions in human prostate cancer using next-generation RNA sequencing[J]. Genome Research, 2011, 21(1): 56-67.

[54] Nacu S, Yuan W L, Kan Z Y, et al. Deep RNA sequencing analysis of readthrough gene fusions in human prostate adenocarcinoma and reference samples[J]. BMC Medical Genomics, 2011, 4: 11.

[55] Ren S C, Peng Z Y, Mao J H, et al. RNA-seq analysis of prostate cancer in the Chinese population identifies recurrent gene fusions, cancer-associated long noncoding RNAs and aberrant alternative splicings[J]. Cell Research, 2012, 22(5): 806-821.

[56] Edgren H, Murumagi A, Kangaspeska S, et al. Identification of fusion genes in breast cancer by paired-end RNA-sequencing[J]. Genome Biology, 2011, 12(1): R6.

[57] Ha K C H, Lalonde E, Li L L, et al. Identification of gene fusion transcripts by transcriptome sequencing in BRCA1-mutated breast cancers and cell lines[J]. BMC Medical Genomics, 2011, 4: 75.

[58] Steidl C, Shah S P, Woolcock B W, et al. MHC class II transactivator CIITA is a recurrent gene fusion partner in lymphoid cancers[J]. Nature, 2011, 471(7338): 377-381.

[59] Scott D W, Mungall K L, Ben-Neriah S, et al. TBL1XR1/TP63: a novel recurrent gene fusion in B-cell non-Hodgkin lymphoma[J]. Blood, 2012, 119(21): 4949-4952.

[60] Pierron G, Tirode F, Lucchesi C, et al. A new subtype of bone sarcoma defined by BCOR-CCNB3 gene fusion[J]. Nature Genetics, 2012, 44(4): 461-466.

[61] Berger M F, Levin J Z, Vijayendran K, et al. Integrative analysis of the melanoma transcriptome[J]. Genome Research, 2010, 20(4): 413-427.

[62] Lawrence M S, Stojanov P, Mermel C H, et al. Discovery and saturation analysis of cancer genes across 21 tumour types[J]. Nature, 2014, 505(7484): 495-501.

[63] Cerami E, Gao J J, Dogrusoz U, et al. The cBio cancer genomics portal: an open platform for exploring multidimensional cancer genomics data[J]. Cancer Discovery, 2012, 2(5): 401-404.

[64] Sawyers C L, Hochhaus A, Feldman E, et al. Imatinib induces hematologic and cytogenetic responses in patients with chronic myelogenous leukemia in myeloid blast crisis: results of a phase II study[J]. Blood, 2002, 99(10): 3530-3539.

[65] Talpaz M, Silver R T, Druker B J, et al. Imatinib induces durable hematologic and cytogenetic responses in patients with accelerated phase chronic myeloid leukemia: results of a phase 2 study[J]. Blood, 2002, 99(6): 1928-1937.

[66] Dienstmann R, Jang I S, Bot B, et al. Database of genomic biomarkers for cancer drugs and clinical targetability in solid tumors [J]. Cancer Discovery, 2015, 5(2): 118-123.

[67] Hastings J F, Latham S L, Kamili A, et al. Memory of stochastic single-cell apoptotic signaling promotes chemoresistance in neuroblastoma[J]. Science Advances, 2023, 9(9): eabp8314.

[68] Siolas D, Hannon G J. Patient-derived tumor xenografts: transforming clinical samples into mouse models[J]. Cancer Research, 2013, 73(17): 5315-5319.

[69] Hidalgo M, Bruckheimer E, Rajeshkumar N V, et al. A pilot clinical study of treatment guided by personalized tumorgrafts in patients with advanced cancer[J]. Molecular Cancer Therapeutics, 2011, 10(8): 1311-1316.

[70] Stebbing J, Paz K, Schwartz G K, et al. Patient-derived xenografts for individualized care in advanced sarcoma[J]. Cancer, 2014, 120(13): 2006-2015.

[71] van Renterghem A W J, van de Haar J, Voest E E. Functional precision oncology using patient-derived assays: bridging genotype and phenotype[J]. Nature Reviews: Clinical Oncology, 2023, 20(5): 305-317.

[72] Jorgensen J H, Ferraro M J. Antimicrobial susceptibility testing: a review of general principles and contemporary practices[J]. Clinical Infectious Diseases, 2009, 49(11): 1749-1755.

[73] Yu M, Bardia A, Aceto N, et al. *Ex vivo* culture of circulating breast tumor cells for individualized testing of drug susceptibility[J]. Science, 2014, 345(6193): 216-220.

[74] Ridky T W, Chow J M, Wong D J, et al. Invasive three-dimensional organotypic neoplasia from multiple normal human epithelia[J]. Nature Medicine, 2010, 16(12): 1450-1455.

[75] Kenny H A, Lal-Nag M, White E A, et al. Quantitative high throughput screening using a primary human three-dimensional organotypic culture predicts *in vivo* efficacy[J]. Nature Communications, 2015, 6: 6220.

[76] Yin S Y, Xi R B, Wu A W, et al. Patient-derived tumor-like cell clusters for drug testing in cancer therapy[J]. Science Translational Medicine, 2020, 12(549): eaaz1723.

[77] Vaira V, Fedele G, Pyne S, et al. Preclinical model of organotypic culture for pharmacodynamic profiling of human tumors [J]. Proceedings of the National Academy of Sciences of the United States of America, 2010, 107(18): 8352-8356.

[78] Nagourney R A, Blitzer J B, Shuman R L, et al. Functional profiling to select chemotherapy in untreated, advanced or metastatic non-small cell lung cancer[J]. Anticancer Research, 2012, 32(10): 4453-4460.

[79] Sachs N, Clevers H. Organoid cultures for the analysis of cancer phenotypes[J]. Current Opinion in Genetics & Development, 2014, 24: 68-73.

[80] Sato T, Vries R G, Snippert H J, et al. Single Lgr5 stem cells build crypt-villus structures *in vitro* without a mesenchymal niche [J]. Nature, 2009, 459(7244): 262-265.

[81] Sato T, Stange D E, Ferrante M, et al. Long-term expansion of epithelial organoids from human colon, adenoma, adenocarcinoma, and Barrett's epithelium[J]. Gastroenterology, 2011, 141(5): 1762-1772.

[82] Boj S F, Hwang C I, Baker L A, et al. Organoid models of human and mouse ductal pancreatic cancer[J]. Cell, 2015, 160(1/2): 324-338.

[83] Gao D, Vela I, Sboner A, et al. Organoid cultures derived from patients with advanced prostate cancer[J]. Cell, 2014, 159(1): 176-187.

[84] Qi F, Li J, Qi Z R, et al. Comprehensive metabolic profiling and genome-wide analysis reveal therapeutic modalities for hepatocellular carcinoma[J]. Research, 2023, 6: 0036.

[85] Launonen I M, Lyytikäinen N, Casado J, et al. Single-cell tumor-immune microenvironment of BRCA1/2 mutated high-grade serous ovarian cancer[J]. Nature Communications, 2022, 13: 835.

[86] Locke D, Hoyt C C. Companion diagnostic requirements for spatial biology using multiplex immunofluorescence and multispectral imaging[J]. Frontiers in Molecular Biosciences, 2023, 10: 1051491.

[87] Taube J M, Roman K, Engle E L, et al. Multi-institutional TSA-amplified multiplexed immunofluorescence reproducibility evaluation (mitre) study[J]. Journal for Immunotherapy of Cancer, 2021, 9(7): e002197.

[88] Ajani J A, Xu Y, Huo L F, et al. YAP1 mediates gastric adenocarcinoma peritoneal metastases that are attenuated by YAP1 inhibition[J]. Gut, 2021, 70(1): 55-66.

[89] Ye G T, Yang Q B, Lei X T, et al. Nuclear MYH9-induced CTNNB1 transcription, targeted by staurosporin, promotes gastric cancer cell anoikis resistance and metastasis[J].

Theranostics, 2020, 10(17): 7545-7560.
[90] Ijsselsteijn M E, Brouwer T P, Abdulrahman Z, et al. Cancer immunophenotyping by seven-colour multispectral imaging without tyramide signal amplification[J]. The Journal of Pathology: Clinical Research, 2019, 5(1): 3-11.
[91] Mori H, Bolen J, Schuetter L, et al. Characterizing the tumor immune microenvironment with tyramide-based multiplex immunofluorescence[J]. Journal of Mammary Gland Biology and Neoplasia, 2020, 25(4): 417-432.
[92] Hoyt C C. Multiplex immunofluorescence and multispectral imaging: forming the basis of a clinical test platform for immuno-oncology[J]. Frontiers in Molecular Biosciences, 2021, 8: 674747.
[93] Eminizer M, Nagy M, Engle E L, et al. Comparing and correcting spectral sensitivities between multispectral microscopes: a prerequisite to clinical implementation[J]. Cancers, 2023, 15(12): 3109.
[94] Skala M C, Deming D A, Kratz J D. Technologies to assess drug response and heterogeneity in patient-derived cancer organoids[J]. Annual Review of Biomedical Engineering, 2022, 24: 157-177.
[95] Xing F Q, Liu Y C, Huang S G, et al. Accelerating precision anti-cancer therapy by time-lapse and label-free 3D tumor slice culture platform[J]. Theranostics, 2021, 11(19): 9415-9430.
[96] Yan Y H, Xing F Q, Cao J Y, et al. Fluorescence intensity and lifetime imaging of lipofuscin-like autofluorescence for label-free predicting clinical drug response in cancer[J]. Redox Biology, 2023, 59: 102578.
[97] Cannon T M, Shah A T, Skala M C. Autofluorescence imaging captures heterogeneous drug response differences between 2D and 3D breast cancer cultures[J]. Biomedical Optics Express, 2017, 8(3): 1911-1925.
[98] Heaster T M, Walsh A J, Zhao Y, et al. Autofluorescence imaging identifies tumor cell-cycle status on a single-cell level[J]. Journal of Biophotonics, 2018, 11(1): e201600276.
[99] Heaster T M, Landman B A, Skala M C. Quantitative spatial analysis of metabolic heterogeneity across *in vivo* and *in vitro* tumor models[J]. Frontiers in Oncology, 2019, 9: 1144.
[100] Lukina M M, Dudenkova V V, Ignatova N I, et al. Metabolic cofactors NAD(P)H and FAD as potential indicators of cancer cell response to chemotherapy with paclitaxel[J]. Acta Biomaterialia, 2018, 1862(8): 1693-1700.
[101] Dugger S A, Platt A, Goldstein D B. Drug development in the era of precision medicine[J]. Nature Reviews Drug Discovery, 2018, 17(3): 183-196.
[102] Guo R, Luo J, Chang J, et al. MET-dependent solid tumours: molecular diagnosis and targeted therapy[J]. Nature Reviews Clinical Oncology, 2020, 17(9): 569-587.
[103] Chrzanowska N M, Kowalewski J, Lewandowska M A. Use of fluorescence *in situ* hybridization (FISH) in diagnosis and tailored therapies in solid tumors[J]. Molecules, 2020, 25(8): 1864.
[104] Pawlyn C, Davies F E. Toward personalized treatment in multiple myeloma based on molecular characteristics[J]. Blood, 2019, 133(7): 660-675.
[105] Treacy P J, Khosla A, Kyprianou N, et al. Value of multiphoton microscopy in uro-oncology: a narrative review[J]. Translational Andrology and Urology, 2023, 12(3): 508-518.
[106] Di Martino J S, Nobre A R, Mondal C, et al. A tumor-derived type III collagen-rich ECM niche regulates tumor cell dormancy[J]. Nature Cancer, 2022, 3(1): 90-107.
[107] Penet M F, Kakkad S, Pathak A P, et al. Structure and function of a prostate cancer dissemination-permissive extracellular matrix [J]. Clinical Cancer Research, 2017, 23(9): 2245-2254.
[108] Ouellette J N, Drifka C R, Pointer K B, et al. Navigating the collagen jungle: the biomedical potential of fiber organization in cancer[J]. Bioengineering, 2021, 8(2): 17.
[109] Zhou Z H, Ji C D, Xiao H L, et al. Reorganized collagen in the tumor microenvironment of gastric cancer and its association with prognosis[J]. Journal of Cancer, 2017, 8(8): 1466-1476.
[110] Best S L, Liu Y M, Keikhosravi A, et al. Collagen organization of renal cell carcinoma differs between low and high grade tumors[J]. BMC Cancer, 2019, 19(1): 490.
[111] 薄启宇, 吴宇辰, 邱斯奇, 等. 三次谐波显微成像在肿瘤诊断中的应用进展[J]. 中国激光, 2024, 51(3): 0307101.
Bo Q Y, Wu Y C, Qiu S Q, et al. Current progress of third harmonic generation microscopy in tumor diagnosis[J]. Chinese Journal of Lasers, 2024, 51(3): 0307101.
[112] 刘风翔, 张礼豪, 黄霞. 拉曼光谱技术在肿瘤诊断中的应用[J]. 激光与光电子学进展, 2022, 59(6): 0617016.
Liu F X, Zhang L H, Huang X. Application of Raman spectroscopy in cancer diagnosis[J]. Laser & Optoelectronics Progress, 2022, 59(6): 0617016.
[113] Duncan M D, Reintjes J, Manuccia T J. Scanning coherent anti-Stokes Raman microscope[J]. Optics Letters, 1982, 7(8): 350-352.
[114] Freudiger C W, Min W, Saar B G, et al. Label-free biomedical imaging with high sensitivity by stimulated Raman scattering microscopy[J]. Science, 2008, 322(5909): 1857-1861.
[115] Du J J, Su Y P, Qian C X, et al. Raman-guided subcellular pharmaco-metabolomics for metastatic melanoma cells[J]. Nature Communications, 2020, 11(1): 4830.
[116] Tan Y Y, Li J J, Zhao G Y, et al. Metabolic reprogramming from glycolysis to fatty acid uptake and beta-oxidation in platinum-resistant cancer cells[J]. Nature Communications, 2022, 13: 4554.
[117] Li J J, Condello S, Thomes-Pepin J, et al. Lipid desaturation is a metabolic marker and therapeutic target of ovarian cancer stem cells [J]. Cell Stem Cell, 2017, 20(3): 303-314.
[118] Cutshaw G, Hassan N, Uthaman S, et al. Monitoring metabolic changes in response to chemotherapies in cancer with Raman spectroscopy and metabolomics[J]. Analytical Chemistry, 2023, 95(35): 13172-13184.
[119] Chen X, Wu Z Q, He Y X, et al. Accurate and rapid detection of peritoneal metastasis from gastric cancer by AI-assisted stimulated Raman molecular cytology[J]. Advanced Science, 2023, 10(21): e2300961.
[120] Kobayashi-Kirschvink K J, Comiter C S, Gaddam S, et al. Prediction of single-cell RNA expression profiles in live cells by Raman microscopy with Raman2RNA[J/OL]. Nature Biotechnology, 2024: 1[2024-01-05]. https://www.nature.com/articles/s41587-023-02082-2#citeas.
[121] Li Z L, Li S W, Zhang S L, et al. Coherent Raman scattering microscopy technique and its biomedical applications[J]. Chinese Journal of Lasers, 2020, 47(2): 0207005.
[122] Zhang B H, Guo L, Yao L, et al. Rapid histological imaging using stimulated Raman scattering microscopy[J]. Chinese Journal of Lasers, 2020, 47(2): 0207018.
[123] Bentley J N, Ji M B, Xie X S, et al. Real-time image guidance for brain tumor surgery through stimulated Raman scattering microscopy[J]. Expert Review of Anticancer Therapy, 2014, 14(4): 359-361.
[124] Yue S H, Li J J, Lee S Y, et al. Cholesteryl ester accumulation induced by PTEN loss and PI3K/AKT activation underlies human prostate cancer aggressiveness[J]. Cell Metabolism, 2014, 19(3): 393-406.
[125] Hong S L, Chen T, Zhu Y T, et al. Live-cell stimulated Raman scattering imaging of alkyne-tagged biomolecules[J]. Angewandte Chemie International Edition, 2014, 53(23): 5827-5831.
[126] Wei L, Hu F H, Shen Y H, et al. Live-cell imaging of alkyne-tagged small biomolecules by stimulated Raman scattering[J]. Nature Methods, 2014, 11(4): 410-412.
[127] Shen Y H, Zhao Z L, Zhang L Y, et al. Metabolic activity induces membrane phase separation in endoplasmic reticulum[J]. Proceedings of the National Academy of Sciences of the United States of America, 2017, 114(51): 13394-13399.
[128] Wei L, Shen Y H, Xu F, et al. Imaging complex protein metabolism in live organisms by stimulated Raman scattering

microscopy with isotope labeling[J]. ACS Chemical Biology, 2015, 10(3): 901-908.
[129] Wei L, Yu Y, Shen Y H, et al. Vibrational imaging of newly synthesized proteins in live cells by stimulated Raman scattering microscopy[J]. Proceedings of the National Academy of Sciences of the United States of America, 2013, 110(28): 11226-11231.
[130] Shen Y H, Xu F, Wei L, et al. Live-cell quantitative imaging of proteome degradation by stimulated Raman scattering[J]. Angewandte Chemie International Edition, 2014, 53(22): 5596-5599.
[131] Hu F H, Chen Z X, Zhang L Y, et al. Vibrational imaging of glucose uptake activity in live cells and tissues by stimulated Raman scattering[J]. Angewandte Chemie (International Ed. in English), 2015, 54(34): 9821-9825.
[132] Long R, Zhang L Y, Shi L Y, et al. Two-color vibrational imaging of glucose metabolism using stimulated Raman scattering [J]. Chemical Communications, 2018, 54(2): 152-155.
[133] Zhang L Y, Shi L Y, Shen Y H, et al. Spectral tracing of deuterium for imaging glucose metabolism[J]. Nature Biomedical Engineering, 2019, 3(5): 402-413.
[134] Liu X W, Shi L X, Zhao Z L, et al. VIBRANT: spectral profiling for single-cell drug responses[J]. Nature Methods, 2024, 21(3): 501-511.
[135] Zhang D L, Li C, Zhang C, et al. Depth-resolved mid-infrared photothermal imaging of living cells and organisms with submicrometer spatial resolution[J]. Science Advances, 2016, 2 (9): e1600521.
[136] He H J, Yin J Z, Li M S, et al. Mapping enzyme activity in living systems by real-time mid-infrared photothermal imaging of nitrile chameleons[J]. Nature Methods, 2024, 21(2): 342-352.
[137] Liu J, Irudayaraj J M K. Non-fluorescent quantification of single mRNA with transient absorption microscopy[J]. Nanoscale, 2016, 8(46): 19242-19248.
[138] 杨朝雁, 赵书瑾, 王子烨, 等. 基于功能化水凝胶的肿瘤源性外泌体高灵敏检测[J]. 光学学报, 2023, 43(21): 2117001.
Yang Z Y, Zhao S J, Wang Z Y, et al. Functionalized hydrogel for highly sensitive detection of tumor-derived exosomes[J]. Acta Optica Sinica, 2023, 43(21): 2117001.

Optical Microscopy Imaging Contributes to Precision Oncology

Yang Bin, Yue Shuhua, Wang Pu*

Beijing Advanced Innovation Center for Biomedical Engineering, School of Biological Science and Medical Engineering, Beihang University, Beijing 100083, *China*

Abstract

Significance Precision oncology is imperative for accommodating the distinct journey of each cancer patient, which is determined by the unique genetic, molecular, and cellular profiles of individual tumors. This shift from a general treatment model to a personalized approach is driven by the recognition that each patient with cancer presents a distinct set of challenges that must be addressed to achieve optimal therapeutic outcomes and prognostic accuracy. The conventional methods of cancer treatment, which typically involve generalized therapies, are deficient owing to the heterogeneity of tumors and the dynamic nature of cancer progression.

The complexity of tumor biology is a multifaceted challenge that is governed by the intricate relationship among genetic mutations, epigenetic alterations, and the tumor microenvironment. Tumors are not static—they evolve through a series of genetic and epigenetic changes that enables them to evade the host's immune system and resist the effects of various treatments. The tumor microenvironment, which comprises a diverse array of cell types, extracellular matrix components, and signaling molecules, significantly affect tumor growth, metastasis, and response to therapy. This renders it difficult to develop comprehensive treatment plans that can effectively target the specific characteristics of each tumor.

Optical microscopy imaging technologies have been adopted widely in precision oncology as they can address the challenges posed by the complexity of tumor biology. These technologies allow one to visualize and analyze tumor tissues and cells with high resolution, thus enabling quantitative and spatially localized analysis of genomic, proteomic, and metabolomic information. This level of detail is critical for identifying patient-specific molecular characteristics and biochemical abnormalities for developing targeted treatment strategies.

The significance of optical microscopy imaging in precision oncology is manifold. First, it bridges the difference between the genomic and phenotypic aspects of cancer, thus allowing for a more nuanced understanding of tumor behavior and response to therapy. Second, it enables the identification of biomarkers that can predict treatment response, thus providing guidance in selecting the most appropriate treatments for individual patients. Third, the non-invasive nature of these imaging techniques allows for the repeated monitoring of tumor progression and response to treatment, thereby facilitating real-time adjustments to treatment strategies as necessary.

The potential of optical microscopy imaging to transform cancer treatment is substantial. By providing detailed, patient-specific information, these imaging techniques can facilitate the development of more effective and less-toxic treatment regimens. This personalized approach can improve patient outcomes by increasing the efficacy of therapies and reducing the incidence of adverse effects. Furthermore, the ability to monitor treatment response in real time can facilitate more informed clinical decision-making, thus potentially improving the overall survival rates and quality of life of patients with cancer.

In conclusion, the integration of optical microscopy imaging into precision oncology is a significant advancement in cancer treatment. Optical microscopy imaging technologies are effective for understanding the complex biology of tumors and for guiding the

development of personalized treatment strategies. As research in this field continues to progress, the potential for optical microscopy imaging to revolutionize cancer diagnosis and treatment will be immense, thus affording more targeted therapies and better patient outcomes in the future. The continued evolution of these technologies is crucial for bridging the disparity between genomic research and clinical practice, thus ultimately resulting in more effective and personalized cancer treatments.

Progress Optical microscopy imaging techniques have progressed significantly in the field of precision oncology and can provide a comprehensive view of tumor characteristics. Auto-fluorescence (AF) imaging has been utilized to monitor metabolic activities within tumors and offers label-free insights into drug responses and cellular metabolism (Fig. 5). Second harmonic generation (SHG) imaging has been pivotal for analyzing the extracellular matrix (ECM), particularly collagen fiber organization, which is crucial for understanding tumor invasion and metastasis (Fig. 7). Coherent Raman scattering (CRS), in particular stimulated Raman scattering (SRS), has emerged as an effective tool for imaging tumor metabolites without requiring labels. SRS has been instrumental in revealing metabolic heterogeneity, which is vital for identifying therapeutic targets and understanding cancer-cell metabolism (Fig. 8). Mid-infrared photothermal (MIP) imaging has demonstrated its potential in assessing drug pharmacokinetics and pharmacodynamics by imaging the distribution of drugs within cells and tissues at a deep cellular level (Fig. 9). Furthermore, multiplex immunofluorescence (mIF) and fluorescence *in situ* hybridization (FISH) have been employed for immunophenotyping (Fig. 4) and genetic analysis (Fig. 6), respectively, to characterize the immune microenvironment and detect gene amplifications. These techniques, as summarized in Table 1, collectively contribute to the increasing number of tools available for the characterization of tumors and the optimization of targeted therapies, thus ultimately improving patient outcomes in cancer treatment.

Conclusions and Prospects Optical microscopy imaging is becoming essential in precision oncology as it allows one to understand the relationship between tumor genetics and phenotypes. As the field progresses, the integration of these imaging techniques into clinical settings will become more evident, which will significantly improve cancer diagnostics and treatment. Future studies shall be conducted to render this technology more accessible by reducing equipment costs and enhancing imaging methodologies, thereby solidifying its key role in precision oncology.

Key words precision oncology; next-generation sequencing; phenotypic functional assays; optical microscopy imaging; coherent Raman scattering; mid-infrared photothermal imaging